

DOI: 10.1002/cssc.201200572

Towards Alternatives to Anodic Water Oxidation: Basket-Handle Thiolate Fe^{III} Porphyrins for Electrocatalytic Hydrocarbon Oxidation

Peiyi Li, Khalaf Alenezi, Saad K. Ibrahim, Joseph A. Wright, David L. Hughes, and Christopher J. Pickett*^[a]

Selective electrocatalytic oxidation of hydrocarbons to alcohols, epoxides or other (higher value) oxygenates should in principal present a useful complementary anodic half-cell reaction to cathodic generation of fuels from water or CO₂ viz. an alternative to oxygen evolution. A series of new basket-handle thiolate Fe^{III} porphyrins have been synthesised and shown to

mediate anodic oxidation of hydrocarbons, specifically adamantane hydroxylation and cyclooctene epoxidation. We compare yields obtained by electrochemical and chemical oxidation of the thiolate porphyrins and benchmark their behaviour against that of Fe^{III} tetraphenyl porphyrin chloride and its tetrapentafluorophenyl analogue.

Introduction

The cathodic generation of fuels, such as dihydrogen from water or carbon monoxide, formate, methanol or other feedstocks from CO₂ using sunlight, wind or other sustainable energy sources, could ameliorate fossil fuel dependency. The complementary anode reaction is usually water oxidation which gives benign, non-polluting dioxygen, but this has little intrinsic value as a co-product. It is, therefore, of interest to consider alternative anode chemistries, particularly those that can employ earth-abundant electrocatalysts rather than unsustainable platinum materials, currently the best material for electrochemical water oxidation.

Alternative reactions to dioxygen evolution should meet the following demands: i) higher value products should be produced from an oxidisable substrate—the electron source; ii) such complementary reactions should give products that are required at a scale comparable to that of solar fuel or feedstock; iii) ideally, the anode chemistry should have fast kinetics and iv) low overpotential. The conversion of hydrocarbons to oxygenates such as alcohols or epoxides could in principle satisfy the first two requirements, the third and fourth demand challenging new chemistry.

Iron porphyrin systems with high-valent ferryl moieties generated by chemical oxygen atom transfer have been extensively studied as functional cytochrome P450 analogues and have been shown to catalyse oxygenation of alkanes and alkenes.^[1] The demonstration of anodic oxidation of hydrocarbons using iron porphyrin electrocatalysts is very limited. To the best of our knowledge, there is only a single report on the oxidation of an alkane by an iron porphyrin:^[2] very little detail is provided; critically, current yields are not given. Similarly, studies on electrochemical alkene oxidation are confined to a single report^[3] and the source of [O] for the oxygenation is not clear beyond a single turnover.

Herein, we describe the synthesis of new iron porphyrin electrocatalysts, which possess an axial thiolate ligand, and the

electrocatalytic activity of these novel molecules in hydrocarbon oxidation. As is seen in the cytochrome P450 enzymes,^[4] these synthetic iron porphyrins possess the structurally robust axial thiolate coordination, which is provided by a basket-handle arrangement^[5] in our systems.^[6] The rigid basket-handle may also provide steric protection of the S-ligand from oxidative degradation. The natural and synthetic catalyst systems are understood to operate via the formation of an oxoferryl porphyrin radical cation, which abstracts a hydrogen atom from hydrocarbon C–H.^[7] It would appear that there are two principal indicators of the reactivity of the active species, the oxidation potential E^0 necessary to access the oxoferryl porphyrin radical cation species and the pK_a of the Fe^{IV}–OH intermediate formed by hydrogen-atom abstraction.^[8] Electron-withdrawing groups on the porphyrin ring increase the oxidising power of the ferryl porphyrin radical cation and this is reflected by a more positive E^0 . On the other hand, a more electron-donating group in the axial position will increase the O–H bond strength by increasing the pK_a . We have explored this balance by synthesising the range of iron porphyrin precursors shown in Figure 1, which possess electron-donating and -withdrawing substituent groups. We compare the electrocatalytic behaviour of these molecules in hydrocarbon oxidation against that in chemical catalysis, where the chemical oxygen atom transfer reagent, iodosylbenzene (PhIO), was employed.

[a] Dr. P. Li, K. Alenezi, Dr. S. K. Ibrahim, Dr. J. A. Wright, Dr. D. L. Hughes, Prof. C. J. Pickett
Energy Materials Laboratory, School of Chemistry
University of East Anglia, Norwich Research Park
Norwich NR4 7TJ (United Kingdom)
Fax: (+44) 1603-592003
E-mail: c.pickett@uea.ac.uk

Supporting Information for this article is available on the WWW under <http://dx.doi.org/10.1002/cssc.201200572>.

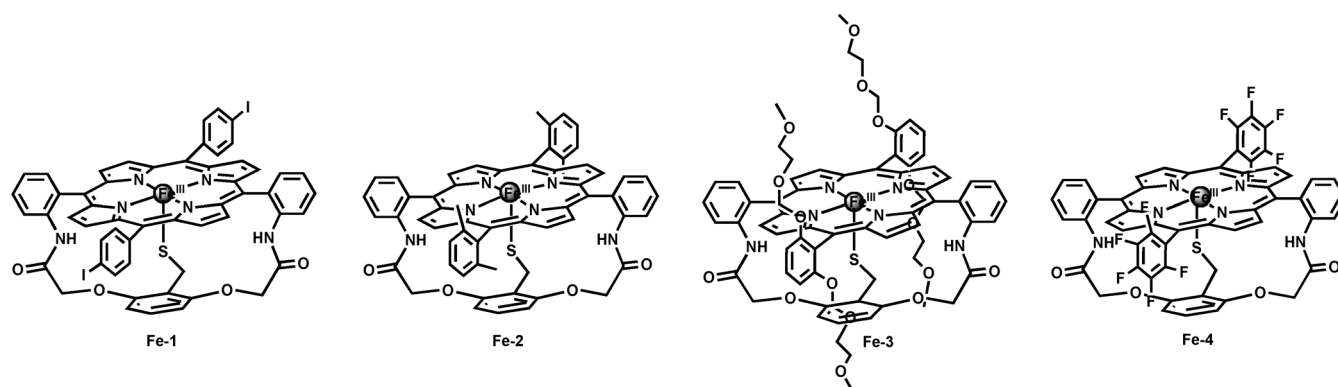


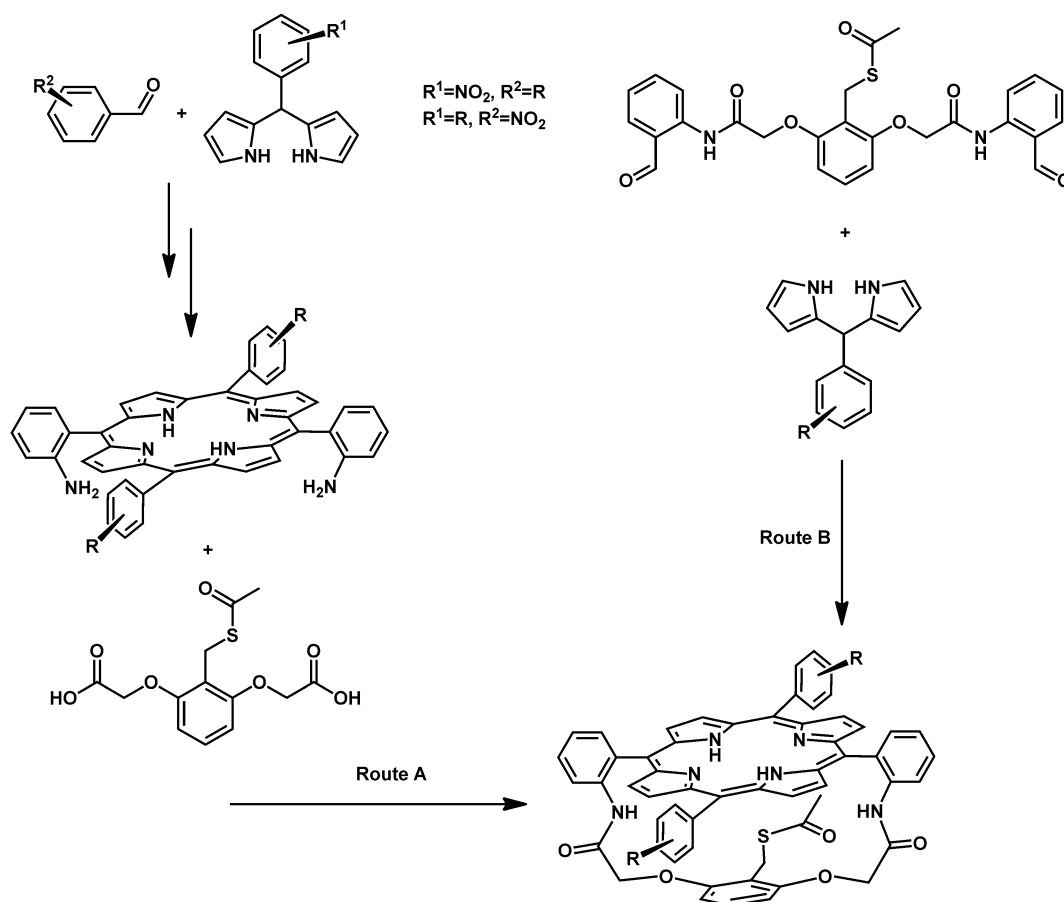
Figure 1. Molecular structures of basket-handle thiolate Fe^{III} porphyrins.

Results and Discussion

Synthesis and structure

A 2,6-dialkoxy benzylthiolate has been chosen as the central component of the strap because the alkoxy functionality enhances the donicity of the benzylthiolate ligand (Scheme 1). The air-sensitive thiolate was protected by an acetyl group as benzyl thioacetate throughout the syntheses and was depro-

tected in the last step after iron insertion. The central 2,6-dialkoxy benzyl thioacetate unit was connected to the main porphyrin body through the formation of two amide bonds. The length of the strap was designed to be just flexible enough to allow the coordination of thiolate to the iron centre. Such an arrangement introduced some rigidity into the strap, which may enhance the stability of thiolate Fe^{III} porphyrins. The strapped porphyrins 1(Ac)–4(Ac) were synthesised by following



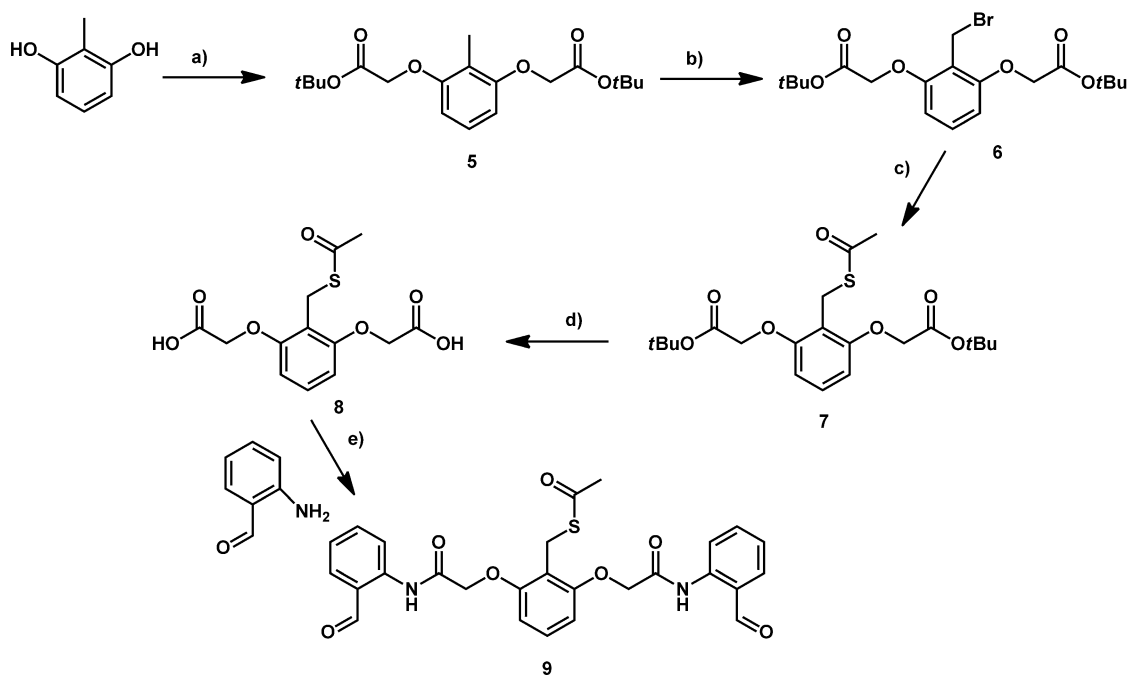
Scheme 1. General strategies for the synthesis of strapped porphyrins 1(Ac)–4(Ac). The side chain R (I, Me, C₆F₅, or polyether) may be introduced by one of two routes.

a classical trifluoroacetic acid (TFA)-catalysed procedure for *trans*-A₂B₂ porphyrins.^[9] Two strategies (Scheme 1, Routes A and B) were employed to synthesise the strapped porphyrin ligands. The first route (Route A) involved two major steps: building the porphyrin body first, followed by attaching the strap to the porphyrin. Alternatively, the strapped porphyrin could be synthesised in a one-pot reaction by condensation of a dipyrromethane with a dialdehyde strap (Route B). Attempts were made to synthesise porphyrins 1(Ac)–3(Ac) via both routes. The yield from each route depended on the peripheral substituents of the porphyrins. Porphyrins 1(Ac) and 2(Ac) were obtained in reasonable yields by Route A, whereas Route B only produced a small amount of impure porphyrins 1(Ac) and 2(Ac). Route A did not generate any porphyrin 4(Ac), which was therefore solely accessed by Route B. Route B was chosen to prepare porphyrin 3(Ac) to avoid the complication from the dealkoxylation of the *meso*-[2,6-bis(2-methoxyethoxy)phenyl] group during the nitro reduction in Route A.

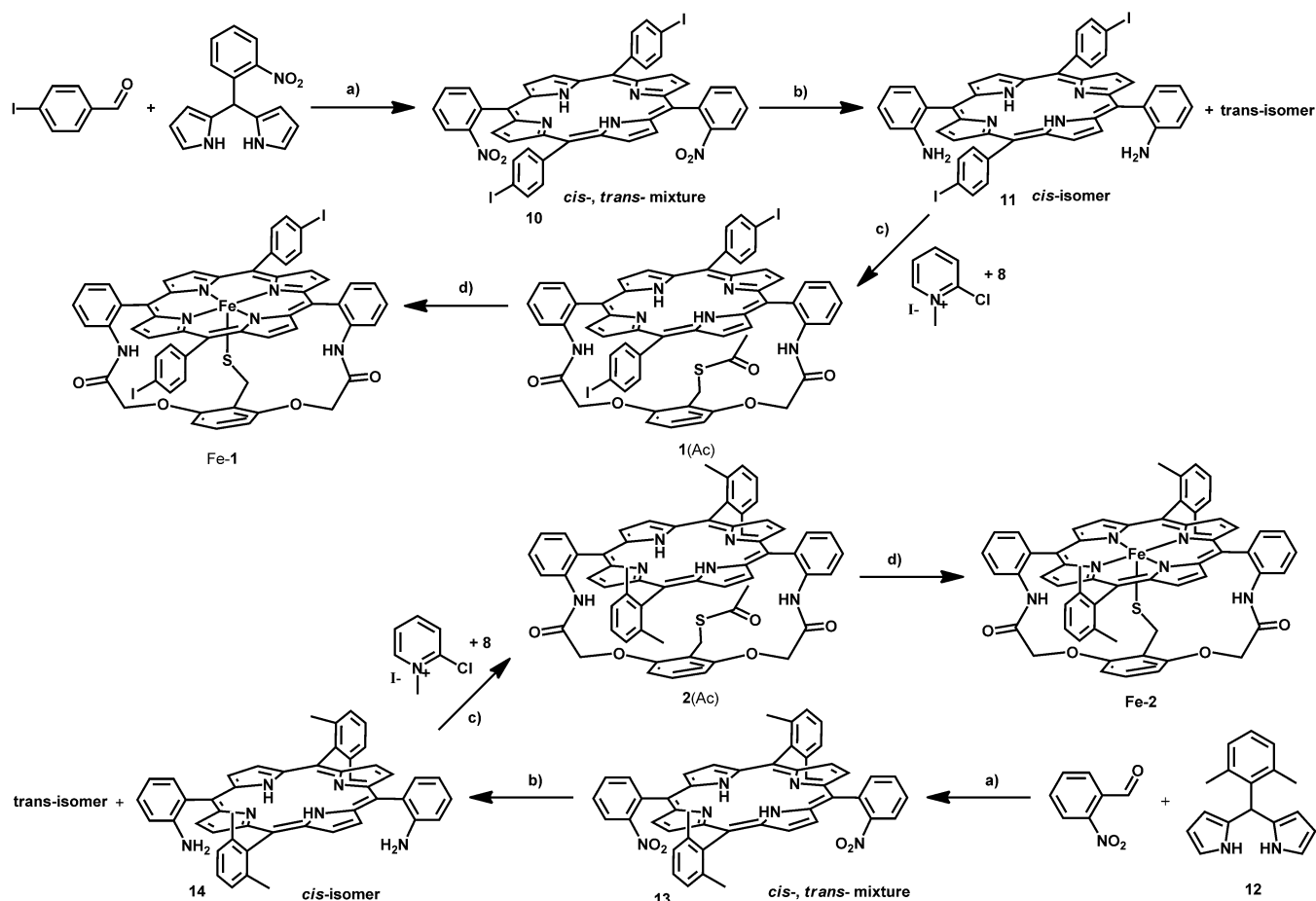
Scheme 2 outlines the synthetic route for the strap linkers 8 and 9. Alkylation of methylresorcinol with *tert*-butyl bromoacetate afforded 2,6-bis(*tert*-butoxycarbonylmethoxy)toluene (5) in an isolated yield of 78%, which was then brominated with *N*-bromosuccinimide (NBS) to produce 1-bromomethyl-2,6-bis(*tert*-butoxycarbonylmethoxy)benzene (6) in an isolated yield of 67%. Treatment of 6 with potassium thioacetate (KSAC) produced thioacetate 7 in an isolated yield of 65%. Deprotection of *tert*-butyl ester within thioacetate 7 with TFA generated dicarboxylic acid 8 in an isolated yield of 82%. The dialdehyde strap linker 9 was prepared by reacting dicarboxylic acid 8 with 2-amino-benzaldehyde with the aid of a Mukaiyama coupling reagent in an isolated yield of 60%.

Porphyrins 1(Ac)–2(Ac) were synthesised in reasonable yields via Route A (Scheme 3). TFA-catalysed condensation of 5-(2-nitrophenyl)dipyrromethane with 4-iodo-benzaldehyde and subsequent oxidation by 2,3-dichloro-5,6-dicyano-1,2-benzoquinone (DDQ) produced the *cis*- and *trans*-isomers of nitro precursor 10 in an isolated yield of 11%. The latter was reduced to amino precursors by SnCl₂ in HCl. The desired *cis*-isomer 11 was separated from the mixture of atropisomers using silica column chromatography. Porphyrin 1(Ac) was prepared in an isolated yield of 70% by coupling 11 with dicarboxylic acid strap linker 8 using a Mukaiyama coupling reagent. A similar approach was adopted to synthesise porphyrin 2(Ac). The nitro precursor 13 (*cis*- and *trans*-isomers) was synthesised by TFA-catalysed condensation of 5-(2,6-dimethylphenyl)dipyrromethane 12 with 2-nitrobenzaldehyde and subsequent oxidation by DDQ in an isolated yield of 11.6%. Reduction of the *cis*/*trans*-mixture of 13 by SnCl₂ in HCl led to a mixture of atropisomers of the amino precursor, from which the desired *cis*-isomer 14 was separated using silica column chromatography. The latter was coupled to the dicarboxylic acid strap linker 8 via Mukaiyama coupling to afford porphyrin 2(Ac) in an isolated yield of 72%.

Scheme 4 summarises the synthesis of porphyrins 3(Ac) and 4(Ac) via Route B. Reaction of resorcinol with methoxyethoxymethyl chloride (MEMCl) yielded 1,3-bis(2-methoxyethoxy)benzene (15) in an isolated yield of 67%. Formylation of 15 with *n*BuLi and DMF furnished 2,6-bis(2-methoxyethoxy)benzaldehyde (16) in an isolated yield of 58%. TFA-catalysed condensation of aldehyde 16 with pyrrole gave dipyrromethane 17 in an isolated yield of 39%. Porphyrin 3(Ac) was then synthesised by TFA-catalysed condensation of dipyrromethane 17 with dialdehyde strap linker 9 and subsequent oxidation by DDQ.



Scheme 2. Synthesis of the strap linkers 8 and 9. Reagents and conditions: a) i) K₂CO₃, acetone, reflux; ii) *tert*-butyl bromoacetate, acetone, reflux; b) NBS, benzoyl peroxide, CCl₄, reflux; c) KSAC, acetone, RT; d) TFA, DCM, RT; e) 2-chloro-1-methylpyridinium iodide, Et₃N, DCM, RT.



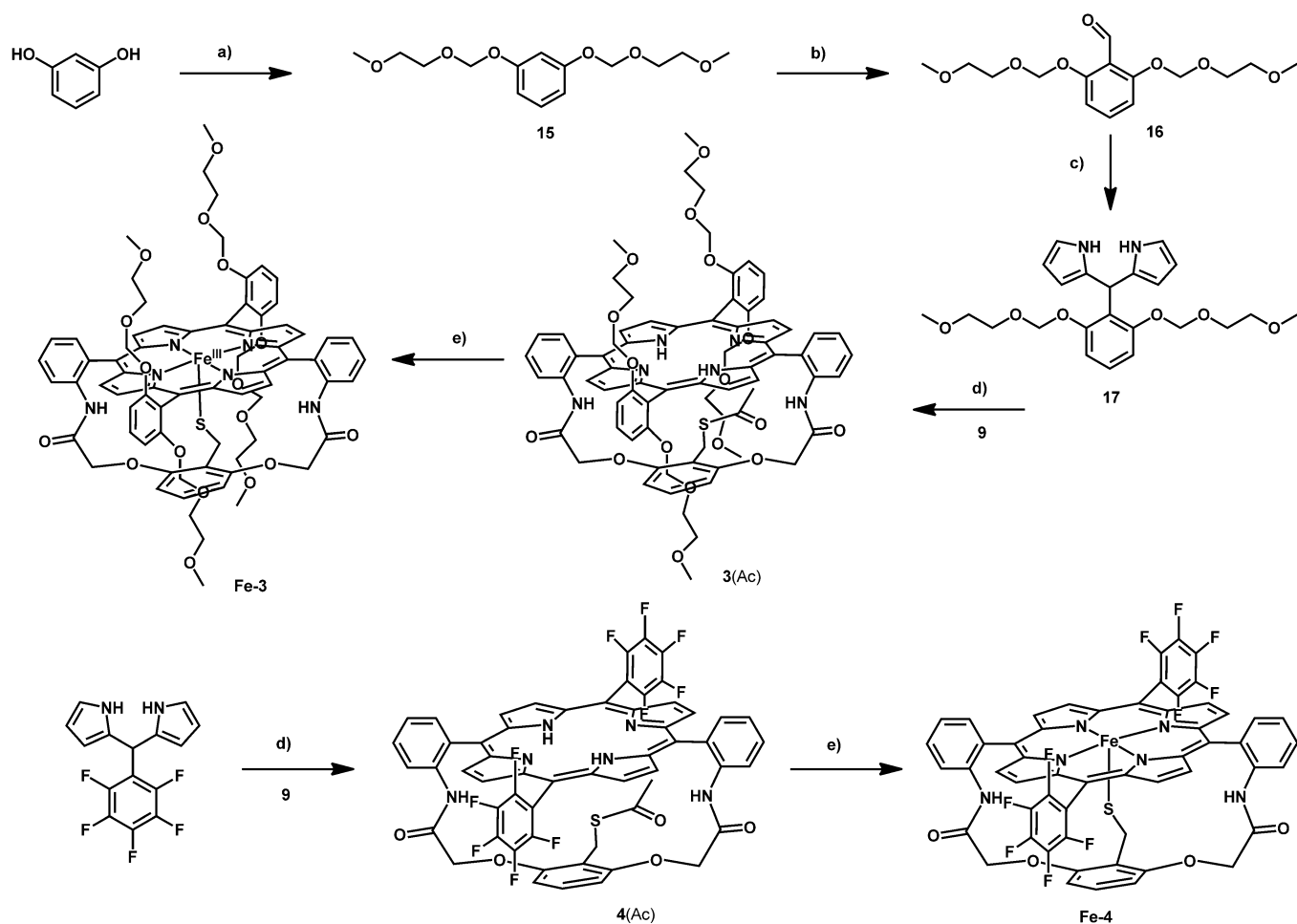
Scheme 3. Synthesis of the strapped thiolate iron porphyrins Fe-1 and Fe-2. Reagents and conditions: a) i) TFA, DCM, RT; ii) DDQ, RT; iii) Et₃N, RT; b) SnCl₂, HCl(aq), RT; c) **8**, Et₃N, DCM, RT; d) i) FeBr₂, lutidine, toluene, reflux; ii) NaOCH₃, RT.

Here, the concentration of the reactants is important as dimerisation occurred at high concentrations and reaction rates and yields were compromised at low concentrations. A series of experiments were carried out under various reactant concentrations, ranging from 0.36 to 3.66 mM for dialdehyde strap linker **9**. The best yield was achieved with a concentration of 2.88 mM for **9** in an isolated yield of 2.3%. The same reactant concentration was employed in the synthesis of porphyrin **4(Ac)**. Coupling of 5-(pentafluorophenyl)-dipyromethane with dialdehyde strap linker **9** in the presence of TFA and subsequent oxidation by DDQ provided porphyrin **4(Ac)** in an isolated yield of 6.6%.

Evidence for the strapped porphyrin is found in the ¹H NMR spectrum as the strap is constrained right under (or above) the porphyrin plane. The CH₂S resonance is not observed at the usual $\delta = 4.3\text{--}4.9$ ppm, but is extremely shielded by the ring current of porphyrin to appear at $\delta = -2.3$ to -2.6 ppm. The monomeric structures of four porphyrins were also supported by their MALDI (matrix-assisted laser desorption/ionization) mass spectra, for which the theoretical isotopic pattern matched exactly with the experimental one (see the Supporting Information). The X-ray crystal structures of **1(Ac)**, **3(Ac)** and **4(Ac)** (Figure 2) also confirm the monomeric structure of

the porphyrin with the strap sitting across the porphyrin plane. Some degree of ruffle deformation exists within all three porphyrins to accommodate the relatively short-length strap containing only eleven atoms. The average displacement of *meso*-carbon attached to the strap from the least-squares 24-atom plane is around 0.5 Å.

There are two ways to reach the final thiolate iron(III) porphyrins Fe-(1–4): iron insertion first, followed by thiol deprotection, or vice versa. Deprotection of the thiol was performed for porphyrin **2(Ac)** in the presence of NaOMe at RT. The resulting mixture was found to contain a moderate amount of decomposed products. As the aerial oxidation of unprotected thiol is facile, the cleavage of the thioacetate group was carried out directly in situ after iron insertion with NaOMe at RT under N₂. The iron insertion into porphyrins **1(Ac)**–**4(Ac)** were accomplished by refluxing porphyrins **1(Ac)**–**4(Ac)** with FeBr₂ and lutidine in toluene (Schemes 3 and 4). Both THF and toluene were tried as solvents, but insertion only reached completion in refluxing toluene. The fast work-up after the reaction allowed iron(II) to be oxidised to iron(III) without significant oxidation of the thiolate sulfur. After purification using silica column chromatography, the desired complexes were crystallised in a CH₂Cl₂/hexane solvent mixture. The isolated yields of iron(III)



Scheme 4. Synthesis of the strapped thiolate iron porphyrins Fe-3 and Fe-4. Reagents and conditions: a) i) NaH, DMF, 0 °C to RT; ii) MEMCl, 0 °C to RT; b) i) *n*BuLi, THF, 0 °C; ii) DMF, 0 °C to RT; c) pyrrole, TFA, RT; d) i) **9**, TFA, DCM, RT; ii) DDQ, RT; iii) Et₃N, RT; e) i) FeBr₂, lutidine, toluene, reflux; ii) NaOCH₃, RT.

porphyrins Fe-1–4) ranged from 50 to 63%. All four thiolate iron porphyrins are stable in air for a brief period, but care should be taken to avoid prolonged exposure, especially in solution.

All four thiolate iron porphyrins are crystalline, but only crystals of Fe-1 and Fe-2 were suitable for X-ray structure analysis. For Fe-2, only the atomic connectivity could be established from the X-ray structure analysis due to the poor data set (Figure 3). It clearly showed that the central iron is coordinated to four nitrogen atoms of the porphyrin and to the sulfur of the benzylthiolate strap. The sixth ligand is the oxygen atom from the amide group of a neighbouring molecule, which has been omitted in Figure 3. The X-ray structure analysis of Fe-1 was good enough to provide a detailed portrait of its structure (Figure 4). Again the porphyrinato core is ruffled, which may be amplified because of the short strap linker. The bending of the porphyrinato core plane toward the strap is clearly shown in the side view of Fe-1 (Figure 4). The central iron is coordinated to the four equatorial nitrogen atoms of the porphyrin, an axial sulfur of benzylthiolate strap and an axial oxygen of a THF solvent molecule.^[10] The average Fe–N bond length is 1.978 Å, with the bond lengths of the axial Fe–

O and Fe–S being 2.205 and 2.163 Å. The octahedral iron is located very close to the plane of the porphyrinato core with only 0.017 Å displacement from the mean 24-atom plane. Overall, the structure is very similar to the ring-anchored benzyl thiolate iron porphyrin reported by Nagano et al.^[11]

In our case, the Fe–S bond length of 2.163(3) Å is slightly shorter than their reported value of 2.1772(12) Å and the 107.4(3)° bond angle of Fe–S–C is not significantly different from Nagano's reported value of 108.26(14)°. It is possible that the rigidity of the constraining strap could be the reason for the slightly shorter Fe–S bond length seen in Fe-1.

Electrochemistry

The electrooxidation of the four new thiolate Fe^{III} porphyrins and the known complexes [Fe(tppf₂₀)Cl] (*meso*-tetrakis(pentafluorophenyl)porphyrin iron(III) chloride) and [Fe(tpp)Cl] (*meso*-tetraphenylporphyrin iron(III) chloride) were studied by using cyclic voltammetry in CH₂Cl₂ containing 0.2 M Bu₄NBF₄ at a vitreous carbon electrode at RT.

Figure 5 shows a set of voltammograms recorded at various scan rates for complex Fe-1. The primary oxidation process is

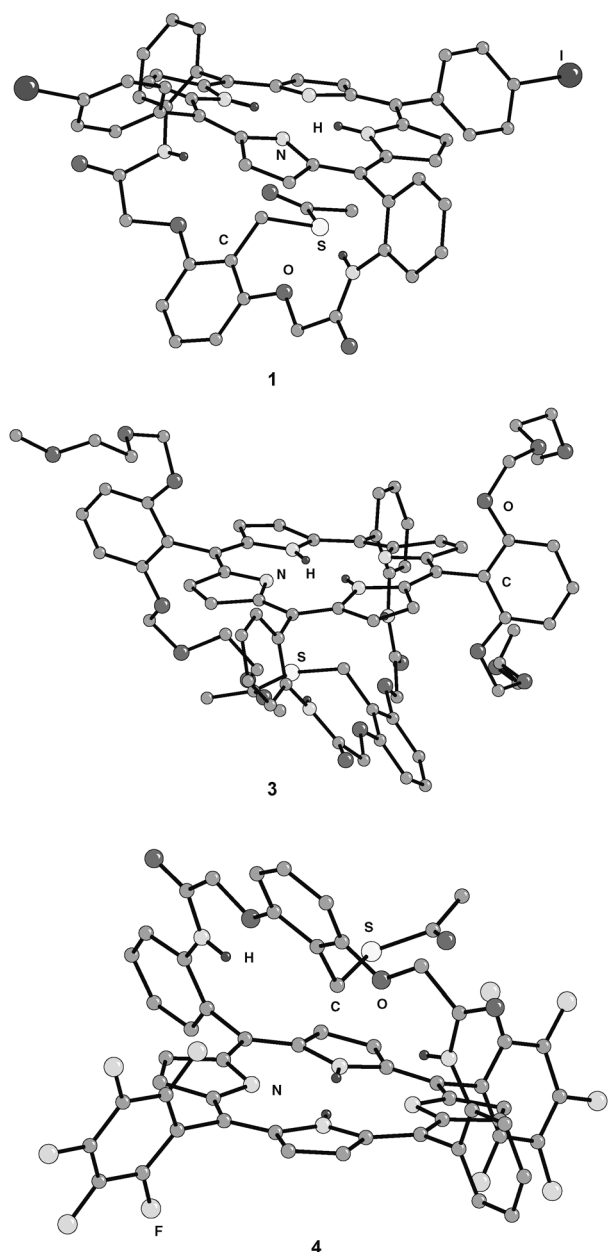


Figure 2. X-ray crystal structures of porphyrins 1(Ac), 3(Ac) and 4(Ac).

a diffusion-controlled reversible one-electron step. Thus: i) the plot of the peak current I_p^{ox} versus $\nu^{1/2}$ is linear with an intercept close to zero (Figure 5, inset a); ii) the magnitude of I_p^{ox} at each scan rate is, as expected, equal to those observed for the primary $Fe^{III/II}$ one-electron reduction process (Figure S1). This first oxidation is probably a metal-centered $Fe^{IV/III}$ -couple, rather than a ligand-based oxidation, because its potential is sensitive to the addition of water/hydroxide as discussed below. Each of the four thiolate complexes shows a similar primary oxidation step (Figure S2). The $E_{1/2}$ values range from 0.76 V versus saturated calomel electrode (SCE) for the most electron-rich porphyrin to 0.96 V versus SCE for the most electron-poor porphyrin (Table 1). The potential for the primary oxidation of the $[Fe(tpp)Cl]$ complex, 1.12 V versus SCE, is ap-

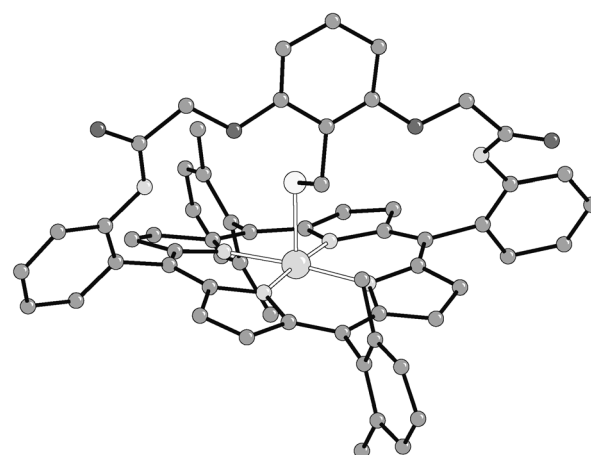


Figure 3. Structure of Fe-2.

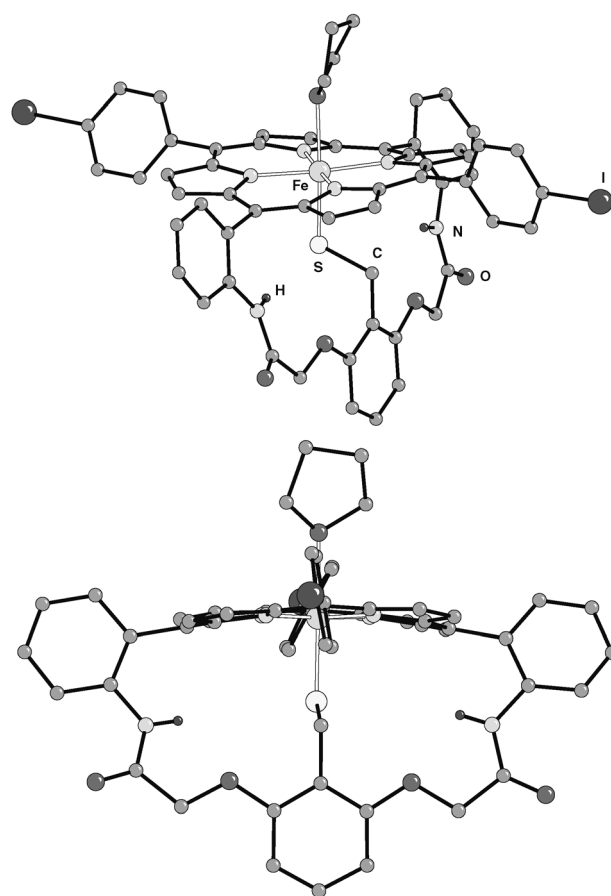


Figure 4. X-ray crystal structure of (THF)Fe-1.

proximately 320 mV more positive than that of Fe-1. This may be a consequence of the better electron-donating ability of the thiolate group compared with Cl, or perhaps more likely a switch from a metal-based oxidation in the case of Fe-1 to a porphyrin-based oxidation, as has been established for $[Fe(tpp)Cl]$.^[12]

Following the primary one-electron oxidation step, a secondary diffusion-controlled process is observed at a more positive potential (I_p^{ox} vs. $\nu^{1/2}$ is linear, Figure 5, inset b). The pro-

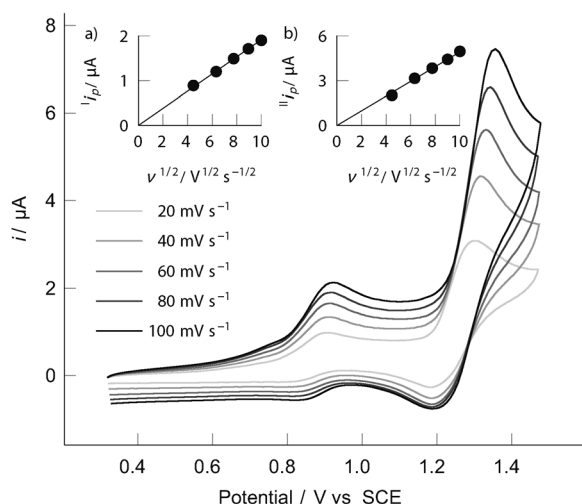


Figure 5. Cyclic voltammograms of Fe-1 at various scan rate in CH_2Cl_2 containing 0.2 M $[\text{Bu}_4\text{N}][\text{BF}_4]$. The inset figures are the plots of $i_p^{\text{ox}2}$ vs. $\nu^{1/2}$.

Table 1. Oxidation potentials (V vs. SCE) in CH_2Cl_2 containing 0.2 M $[\text{Bu}_4\text{N}][\text{BF}_4]$.			
Catalyst	$^1E_{1/2}$ [a]	Potential [V]	$^2E_p^{\text{red}}$ [b]
Fe-1	0.88	1.44	1.21
Fe-2	0.8	1.37	1.19
Fe-3	0.76	1.43	1.17
Fe-4	0.96	1.45	1.29
$[\text{Fe}(\text{tppf}_{20})\text{Cl}]$	1.58 ^[c] /1.48 ^[d]	1.77	1.62
$[\text{Fe}(\text{tpp})\text{Cl}]$	1.12	1.39 ^[e]	1.39 ^[e]

[a] Reversible one-electron process. [b] Irreversible multi-electron process. [c] E_p^{ox} for irreversible two-electron process. [d] E_p^{red} for irreversible one-electron process. [e] Reversible one-electron process, $^2E_{1/2}$.

cess appears partially reversible and the plot of $i_p^{\text{ox}2}$ vs. $i_p^{\text{ox}1}$ is linear with a slope of 2.5 as shown in Figure 6. The expected ratio between the fast reversible two-electron and one-electron systems is $(2n/1n)^{3/2} = 2.83$. However, the ratio of 2.5 that we observe, the peak separation and the overall shape of the voltammogram are best simulated by two consecutive one-electron steps with a following chemical step and further electron transfer increasing the current. The digital simulation and

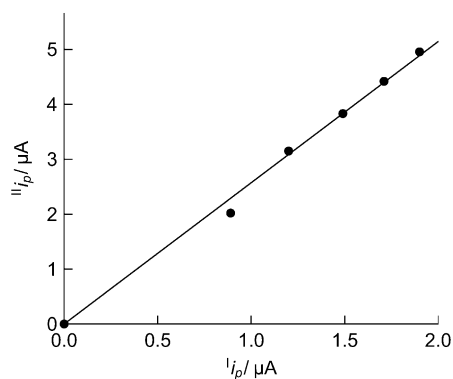


Figure 6. Plots of $i_p^{\text{ox}2}$ versus $i_p^{\text{ox}1}$. Scan rate = 0.1 V s^{-1} .

the experimental voltammogram recorded at 100 mV s^{-1} are shown in Figure S3 and the simulation parameters are also listed in the Supporting Information. The other iron thiolate porphyrins all show similar secondary oxidations as shown in Figure S2; the ratio of $i_p^{\text{ox}2}$ to $i_p^{\text{ox}1}$ at 100 mV s^{-1} in all cases is between 2–3 and must depend upon the kinetics associated with the chemical step.

In preparative electrolyses using the iron porphyrins as electrocatalysts we found that the presence of the strong base $[\text{NBu}_4][\text{OH}] \cdot 30\text{H}_2\text{O}$ was essential for hydrocarbon oxidation in all cases. We have, therefore, examined the effect of this reagent on the cyclic voltammograms of the systems, focusing again on Fe-1. Figure 7a shows the effect of the base at a low

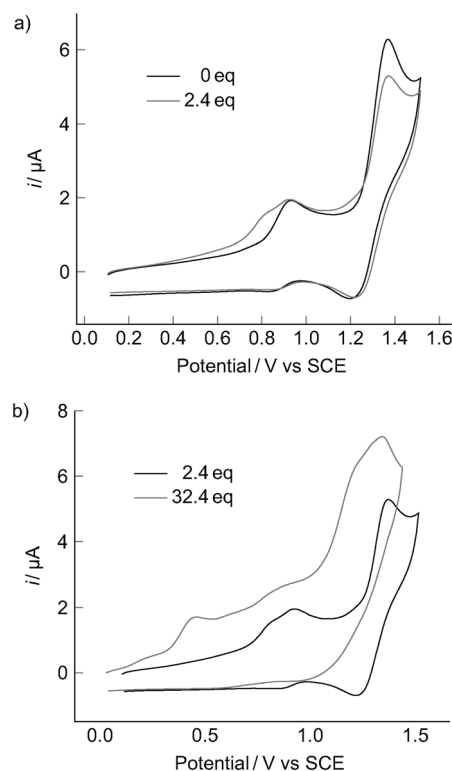


Figure 7. Cyclic voltammograms of Fe-1 in CH_2Cl_2 containing 0.2 M $[\text{Bu}_4\text{N}][\text{BF}_4]$ at RT with added $[\text{Bu}_4\text{N}][\text{OH}]$. Scan rate = 0.1 V s^{-1} .

concentration (2.4 equivalents OH^-) on the cyclic voltammetry. The key features are a negative shift in the potential for the primary oxidation peak by about 120 mV and a reduction in the magnitude of $i_p^{\text{ox}1}$ by about 20%. Figure 7b shows the effect of increasing the reagent concentration approximately 13-fold to 32 equivalents. In this case, we see a new oxidation peak at a relatively low potential with $^{\text{OH}}E_p = 0.43 \text{ V}$ versus SCE, which is accompanied by suppression of the low base/zero base peaks at 0.7–0.9 V versus SCE and a negative shift of the ‘secondary’ oxidation process by about 160 mV. The increase in the ‘low potential’ species with increasing base is shown by Figure 8. We suggest that at low concentrations of the added base speciation is predominately water occupying the axial site and at higher base concentrations the majority species is

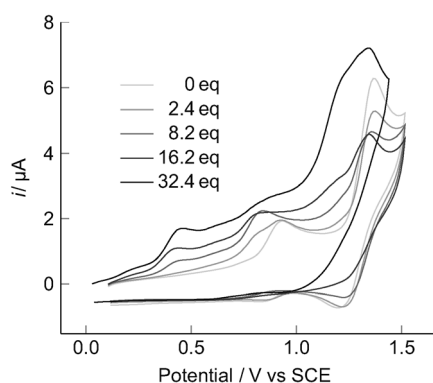


Figure 8. Cyclic voltammograms of Fe-1 in CH_2Cl_2 containing 0.2 M $[\text{Bu}_4\text{N}][\text{BF}_4]$ at RT with various $[\text{Bu}_4\text{N}][\text{OH}]$ concentrations. Scan rate = 0.1 V s^{-1} .

the hydroxide ligated complex, Scheme 5. This would be consistent with the new peak at $E_p = 0.43 \text{ V}$ versus SCE being associated with the hydroxide species whilst that at 0.79 V versus SCE being the aquo species. The irreversibility of the oxidation of the aquo species may be attributed to proton removal by the base; similarly, this may explain the irreversibility of the oxidation of the hydroxide species whereby iron(IV) oxo species are formed (Scheme 5). The lower peak current associated with secondary process in the presence of a base may be attributable to the formation of stable oxo species rather than destructive oxidation of the porphyrin.

Chemical oxidation

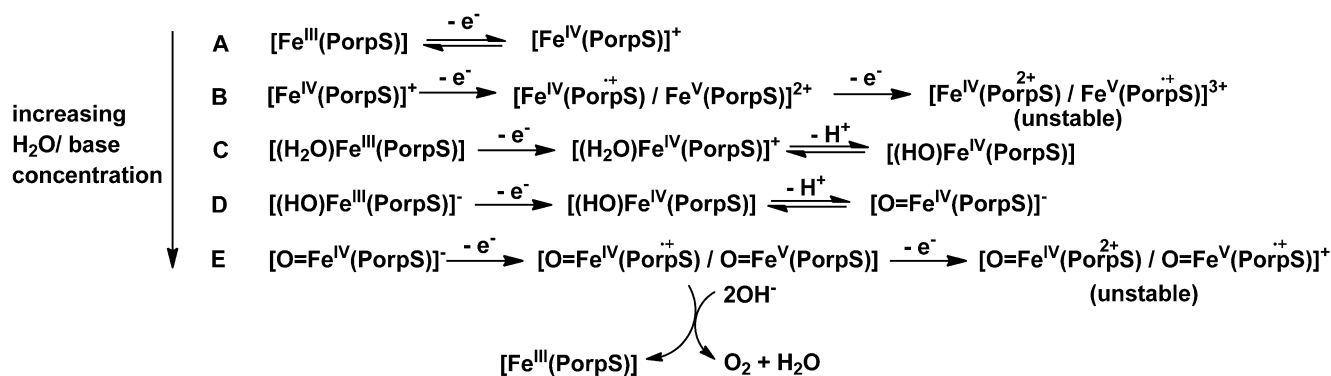
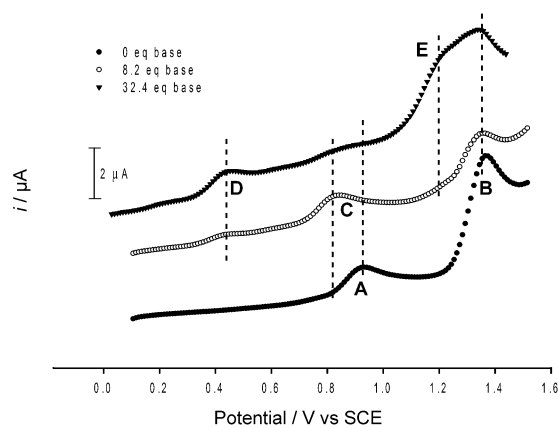
Chemical oxidation of adamantane and cyclooctene using PhIO as an oxygen source was carried out in CH_2Cl_2 at 20°C under N_2 for 1 h. Under our reaction conditions, all iron porphyrins catalysed the oxidation of adamantane and cyclooctene to 1-adamantanol and cyclooctene oxide, respectively, with minimal formation of other hydrocarbon oxidation products (Table 2).

The first and simplest iron porphyrin catalyst $[\text{Fe}(\text{tpp})\text{Cl}]^{[1e]}$ provides a benchmark^[13] against which we can compare hydro-

Table 2. Yields of Fe^{III} porphyrin-catalysed adamantane/cyclooctene oxidations by PhIO.^[a]

Catalyst	1-Adamantanol	TON ^[c]	Cyclooctene oxide	TON ^[c]
	yield [%] ^[b]		yield [%] ^[b]	
Fe-1	22.5	3	70.4	5.2
Fe-2	34.7	2	69.7	5.5
Fe-3	10.5	0.53	66.4	4
Fe-4	43.4	3.2	86.1	6
$[\text{Fe}(\text{tppf}_{20})\text{Cl}]$	60.8	3.7	86.2	7
$[\text{Fe}(\text{tpp})\text{Cl}]$	11.3	0.5	74.7	5.2

[a] Reactions were carried out in CH_2Cl_2 at 20°C under N_2 for 1 h. $[\text{Fe}^{\text{III}}$ porphyrin] = 1.0 mM ; $[\text{PhIO}] = 10 \text{ mM}$; $[\text{adamantane or cyclooctene}] = 0.1 \text{ M}$. [b] Average value of two experiments based on PhIO consumed. [c] TON = moles of product/moles of catalyst. The theoretical maximum TON is 10 based upon ratio of moles of PhIO/moles of catalyst.



Scheme 5. Proposed oxidation steps in absence and presence of a base.

carbon oxidation activity of the new thiolate porphyrins. Table 2 shows that all of the thiolate complexes except Fe-3 have a higher activity than [Fe(tpp)Cl], both in terms of turnover number (TON) and yield of 1-adamantanol. The least electron-rich complex, Fe-4, is the best thiolate-based catalyst, whereas the most electron-rich complex, Fe-3, is the least active. This indicates that electron-withdrawing groups give rise to the most reactive ferryl units.^[14] This electronic effect must override the protection against Fe–O–Fe *m*-oxo dimer formation (deactivation) that we might expect to be afforded by the oligoether chains of Fe-3. An earlier study of the pentafluorophenylporphyrin iron complex^[15] showed a notably high adamantane oxidation activity. In accord with this, we find that [Fe(tppf₂₀)Cl] is the most active catalyst precursor under our conditions: it is correspondingly the hardest to oxidise electrochemically (Table 1). Other than electron density, the geometric arrangement around the thiolate sulfur may also play a role. The electron densities on Fe-1 and Fe-2 are very similar, yet the 1-adamantanol yield employing Fe-2 (34.7%) is significantly higher than that of Fe-1 (22.5%). The four *ortho*-methyl groups in Fe-2 may shield the thiolate ligand from oxidative destruction and/or prevent the formation of the inactive *m*-oxo dimer. Where there is no significant electronic perturbation of the porphyrin ring, as in the cases of Fe-1 and [Fe(tpp)Cl], the sulfur axial ligand must favour hydrogen abstraction from the substrate, as demonstrated by the yield of 1-adamantanol (22.5% for Fe-1 vs. 11.3% for [Fe(tpp)Cl]). In an earlier study, Higuchi et al.^[16] were also able to show that a ring-anchored benzyl thiolate had a substantially better activity than [Fe(tpp)Cl] using a peroxy acid as the oxygen atom source.

With respect to epoxidation of the more reactive cyclooctene, the electronic and geometric effects of the iron porphyrins on the catalytic activity are levelled out, the two most electron deficient iron porphyrins gave the highest yields of approximately 85%, with the other complexes giving yields of about 70% (Table 2).

Electrochemical oxidation of adamantane and cyclooctene

Electrocatalytic oxidations of adamantane and cyclooctene were carried out in wet CH₂Cl₂ at RT under N₂ for 1.5 h using 0.2 M [Bu₄N][BF₄] as the electrolyte and in the presence of tetrabutylammonium hydroxide. Based on the cyclic voltammograms of four thiolate iron porphyrins, [Fe(tppf₂₀)Cl] and [Fe(tpp)Cl], the applied potentials for Fe-1, Fe-2, Fe-3, Fe-4, [Fe(tppf₂₀)Cl] and [Fe(tpp)Cl] were set at 1.36, 1.27, 1.31, 1.42, 1.70 and 1.49 V (vs. SCE), respectively. They are sufficiently positive to ensure accessing the two-electron oxidised state of the Fe^{III} complexes.

It was found that the presence of hydroxide is crucial. Without this base control, experiments show that no adamantanol or cyclooctene oxide is formed. This is consistent with the proposed electrocatalytic mechanism shown in Scheme 6. The iron(III) hydroxide is oxidised by removal of two electrons and a proton, assisted by free base, which thus generates the highly reactive ferryl species. The lower efficiency of electro-

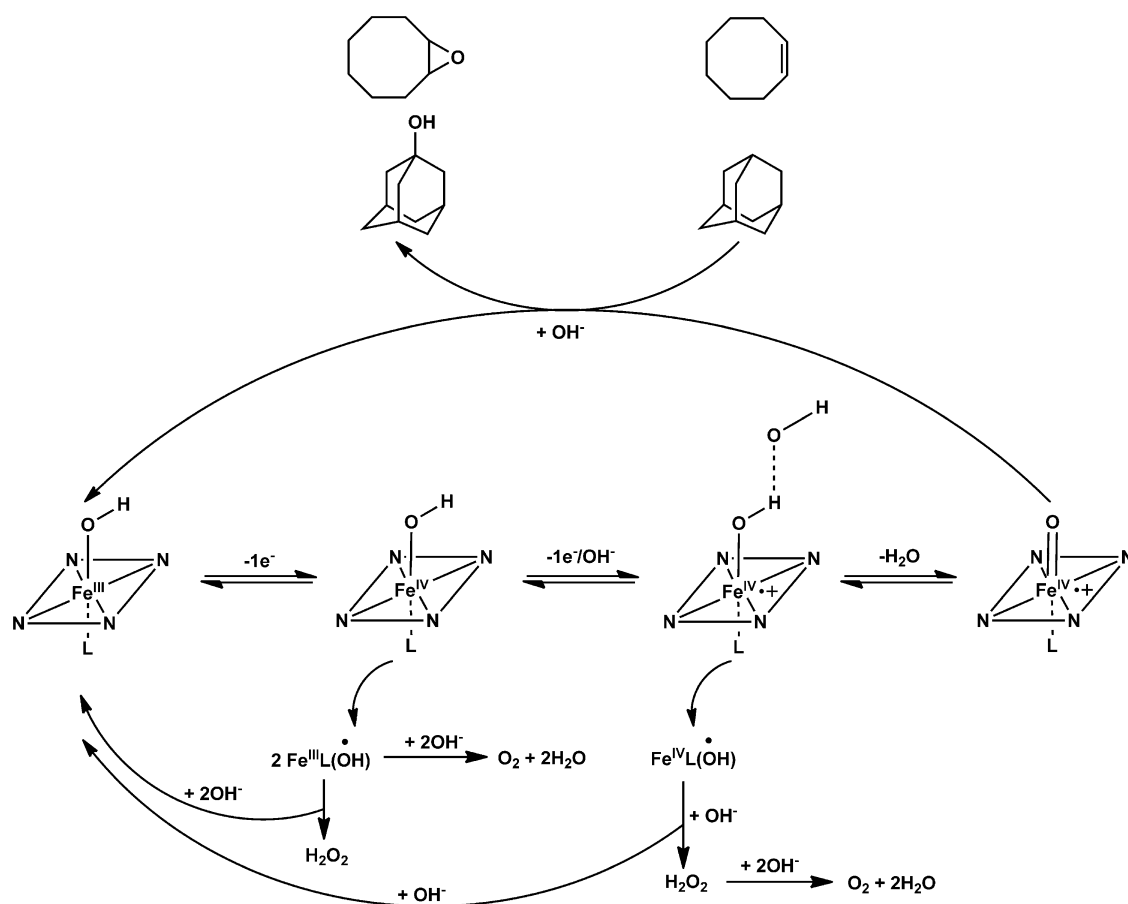
chemical oxidation with respect to chemical oxidation can be ascribed to the competing generation of superoxide, peroxide or dioxygen (Scheme 6). In the absence of an iron porphyrin catalyst, cyclooctene could be electrochemically oxidised to cyclooctene epoxide in the presence of OH⁻ with a current efficiency of 5.6% at an anode potential of 1.8 V (vs. SCE). However, only a trace amount of 1-adamantanol was detected under the same experimental conditions. The applied potential is positive enough to produce OH[•] radicals,^[17] which evidently convert cyclooctene to cyclooctene oxide, probably via peroxide. However, neither of these species are powerful enough to oxidise adamantane to 1-adamantanol to a significant extent. Thus, the presence of iron porphyrins lowers the activation barriers for adamantane hydroxylation and cyclooctene epoxidation, dramatically increasing the current efficiency for their formation and substantially lowering the anode potentials required (Table 3). Notably, the cyclic voltammetry of Fe-1 in the presence of adamantane at high concentration is only marginally perturbed by the substrate, consistent with no direct oxidation. In the presence of the base and the substrate the cyclic voltammogram is largely dominated by the effect of base; consistent with slow hydrocarbon oxidation kinetics, some minor effects on peak currents are observed.

In parallel with the chemical oxidation of adamantane, the electron density on the iron porphyrin appears to be the major factor that determines the current efficiency and turnover number: both increase as the electron density on the iron porphyrin decreases. Thus, among the four thiolate porphyrins, the most electron-deficient Fe-4 provides the highest current efficiency and the most electron rich Fe-3 gives the lowest current efficiency. Again, [Fe(tppf₂₀)Cl] exhibits overall the highest current efficiency whilst [Fe(tpp)Cl] has the lowest. The effect of geometric arrangement around the thiolate sulfur on the current efficiency of electrocatalytic oxidation (9.4% for Fe-1 vs. 9.8% for Fe-3) is not as significant as for that observed for the chemical oxidation (22.5% for Fe-1 vs. 34.7% for Fe-3). This is understandable since the oxidative destruction of the thiolate ligand from a strong oxygen-transfer reagent, such as PhIO, is no longer applicable in the case of electrocatalytic oxidation. The current efficiencies of cyclooctene epoxidation are also shown in Table 3. [Fe(tppf₂₀)Cl] is the best electrocatalyst in terms of current efficiency, but it also operates at the highest oxidation potential.

In general, our basket-handle thiolate complexes are clearly superior to the prototypical [Fe(tpp)Cl] system, both in terms of potential and current efficiency, and further modification might increase the current efficiency without significantly increasing the oxidation potential.

Conclusions

A series of new basket-handle thiolate Fe^{III} porphyrins have been synthesised and fully characterised. We have determined the activity of these porphyrins as catalysts in chemical hydrocarbon oxidations and have benchmarked them against iron tetraphenylporphyrin and its tetrapentafluorophenyl analogue.



Scheme 6. Proposed mechanism of electrocatalytic oxidation of hydrocarbons.

Table 3. Current efficiencies and turnover numbers of electrocatalytic oxidations of adamantane/cyclooctene catalysed by Fe^{III} porphyrins.^[a]

Catalyst	Oxidation potential [V vs. SCE]	1-Adamantanol yield [%] ^[b]	TON ^[c]	Cyclooctene oxide yield [%] ^[b]	TON ^[c]
Fe-1	1.36	9.4	2.7(28.1)	16.1	4.6(28.7)
Fe-2	1.27	9.8	3.0(33.8)	20.9	5.1(24.5)
Fe-3	1.31	2.5	0.7(25.9)	12.5	3.4(27.6)
Fe-4	1.42	14.5	4.1(28.5)	28.2	6.4(22.7)
[Fe(tppf ₂₀)Cl]	1.70	35.8	7.5(29.1)	38.9	12.3(31.4)
[Fe(tpp)Cl]	1.49	2.6	0.8(31.9)	17.4	5.2(24.5)

[a] Reactions were carried out in CH₂Cl₂ at RT under N₂ for 1.5 h. [Fe^{III} porphyrin]=0.45 mM; [Bu₄NOH]=62 mM; [adamantane or cyclooctene]=0.1 M; [Bu₄NBF₄]=0.2 M; [H₂O]=1.8 M. [b] Average value of two experiments. [c] TON=moles of product/moles of catalyst; number in bracket is the theoretical TON. The theoretical maximum TON is based upon the total charge passed (F)/2 mol of catalyst.

Importantly, we show that in principle hydrocarbon oxidation can be driven anodically using these iron porphyrins. We report the first current efficiency data (yields) for this type of electrochemical oxidation. We show that a current efficiency of 36% can be achieved with an iron tetrapentafluorophenylporphyrin electrocatalyst in a dichloromethane electrolyte at +1.7 V versus SCE. Notably, the operating potential can be reduced to approximately +1.4 V versus SCE by using a thiolate ligated iron porphyrin, although at the cost of a lower current

efficiency (14.5%). This work goes some way towards establishing a proof of concept that alternatives to that of water oxidation might usefully be explored in solar fuel/feedstock-generating systems. Lower oxidation potentials and faster kinetics are of course necessary targets.

Experimental Section

Characterization

All NMR spectra were recorded by using a Bruker Avance 300 and referenced to the residual solvent signals. All MALDI mass spectra were acquired by using an Applied Biosystems Voyager DE STR MALDI equipped with linear and reflectron analysers. All high-resolution mass spectra were recorded by using a ThermoFisher LTQ Orbitrap XL.

GC analyses were performed using a Hewlett-Packard 5890 II gas chromatograph equipped with a flame ionization detector (FID) and a 25 m×0.32 mm 5% phenyl/95% dimethylpolysiloxane capillary column (ID-BPX5 1.0). An injection volume of 1 μL was used in all GC analyses. The products were identified by comparing their retention times in GC with those of authentic samples. The yields of oxidation products were determined by comparison against standard curves (bromobenzene was used as an internal standard for adamantane hydroxylation and *n*-dodecane for epoxidation of cyclooctene).

Chemical oxidations were carried out in a sealed Schlenk tube charged with the iron porphyrin catalyst, substrate, PhIO and dry CH_2Cl_2 under N_2 at 20°C for 1 h. The reaction mixture was passed through a short pad of dry Celite to remove unreacted PhIO. The CH_2Cl_2 filtrate was injected directly to a gas chromatographer for product analysis.

Cyclic voltammetric measurements were carried out using an Autolab PGSTAT 30 potentiostat. A conventional three-electrode arrangement was employed, consisting of a vitreous-carbon working electrode, a platinum wire as the auxiliary electrode and SCE as a reference electrode. All measurements were performed in dry CH_2Cl_2 in the presence of 0.2 M tetrabutylammonium tetrafluoroborate as the supporting electrolyte at RT. All solutions were thoroughly degassed with nitrogen prior to being used, and during the measurements a nitrogen atmosphere was maintained. The electrocatalytic hydrocarbon oxidations were performed in a three-electrode and three-compartment cell where adjacent compartments were separated by a glass frit. A vitreous-carbon working electrode was fitted into the central compartment, with the platinum-wire auxiliary electrode and Ag/AgCl (CH_2Cl_2 , 0.5 M $[\text{Bu}_4\text{N}]\text{Cl}$) reference electrode in the adjoining compartments. Fe^{III} porphyrin catalyst, $[\text{Bu}_4\text{N}][\text{OH}]\cdot 30\text{H}_2\text{O}$ base, hydrocarbon substrate and $[\text{Bu}_4\text{N}][\text{BF}_4]$ (total volume 3 mL) electrolyte were added into the working electrode compartment and dissolved in CH_2Cl_2 (3 mL). The auxiliary and reference compartments were charged with a CH_2Cl_2 solution containing $[\text{Bu}_4\text{N}][\text{BF}_4]$ electrolyte (0.2 M). All solutions inside the cell were thoroughly degassed with N_2 and sealed under N_2 prior to use. To avoid damage to the capillary column we found it necessary to remove the supporting electrolyte. This was achieved in the following way. After each electrolysis, CH_2Cl_2 was removed from the solution mixture under a controlled vacuum (42.7 kPa) at RT. This was optimal for removal of the solvent whilst leaving the organic product intact. The residue was then treated with dry diethyl (10 mL) ether to extract the product, leaving insoluble $[\text{Bu}_4\text{N}][\text{BF}_4]$ which was removed by pipette filtration. The filtrate was evaporated under a controlled vacuum (42.7 kPa) to remove diethyl ether. The residue was re-dissolved in dry CH_2Cl_2 (2 mL) with added internal reference. The resulting CH_2Cl_2 solution was then subjected to GC analysis. Control experiments established the efficacy of this extraction procedure.

Materials

All solvents were dried and degassed prior to use. All commercial chemicals were used as received unless otherwise stated. All reactions were carried out under a dry N_2 -atmosphere unless otherwise stated. PhIO was prepared according to a published procedure^[18] and its purity was checked by iodometric titration to be above 99%. Starting materials, 5-(2-nitrophenyl)-dipyrromethane,^[19] 4-iodo-benzaldehyde^[20] and 5-(pentafluorophenyl)-dipyrromethane^[21] were synthesised according to literature procedures.

Synthesis

2,6-Bis(tert-butoxycarbonylmethoxy)toluene (5): K_2CO_3 (16.03 g, 0.116 mol) was added to methylresorcinol (6.00 g, 4.83 mmol) in acetone (200 mL), and the dark red suspension was heated at 60°C for 2 h. The dark red suspension turned light upon addition of *tert*-butyl bromoacetate (15.70 mL, 0.106 mol). The mixture was then refluxed for two days, turning into a white suspension. TLC indicated the reaction was complete. The white suspension was filtered through a short pad of Celite and the filtrate was evaporated at reduced pressure to yield a yellow solid. The crude product was puri-

fied by using silica column chromatography (hexane/EtOAc, 10:1) to afford **5** as a white solid (13.30 g, 78%). $^1\text{H NMR}$ (300 MHz, CDCl_3): $\delta = 1.48$ (s, 18H), 2.23 (s, 3H), 4.51 (s, 4H), 6.40 (d, $J = 8.3$ Hz, 2H), 7.04 ppm (t, $J = 8.3$ Hz, 1H); $^{13}\text{C NMR}$ (300 MHz, CDCl_3): $\delta = 8.63$, 28.17, 66.44, 82.26, 105.28, 116.21, 126.14, 157.11, 168.37 ppm; NSI-HRMS: m/z calcd. for $\text{C}_{19}\text{H}_{28}\text{O}_6\text{NH}_4$: 370.2222 $[\text{M}+\text{NH}_4]^+$, found: 370.2224; elemental analysis calcd. (%) for $\text{C}_{19}\text{H}_{28}\text{O}_6$: C 64.75, H 8.01; found: C 64.88, H 8.13.

1-Bromomethyl-2,6-bis(tert-butoxycarbonylmethoxy)benzene

(6): Compound **5** (13.00 g, 36.9 mmol) was dissolved in CCl_4 (130 mL) before the addition of NBS (7.30 g, 0.041 mol) and benzoyl peroxide (90 mg, 0.372 mmol). The suspension was refluxed overnight, during which time the pale yellow suspension turned yellow-brown; TLC indicated that the reaction was complete. The cooled suspension was filtered through a short pad of Celite, and the filtrate was evaporated in vacuo to yield a brown solid. The crude product was purified by using silica column chromatography (hexane/EtOAc, 10:1) to afford **6** as a colourless oil (10.69 g, 67%). $^1\text{H NMR}$ (300 MHz, CDCl_3): $\delta = 1.47$ (s, 18H), 4.60 (s, 2H), 4.81 (s, 2H), 6.42 (d, $J = 8.4$ Hz, 2H), 7.17 ppm (t, $J = 8.3$ Hz, 1H); $^{13}\text{C NMR}$ (300 MHz, CDCl_3): $\delta = 23.13$, 28.19, 66.52, 82.58, 105.54, 116.23, 129.93, 157.21, 167.86 ppm; ESI-HRMS: m/z calcd. for $\text{C}_{19}\text{H}_{27}\text{BrO}_6\text{NH}_4$: 448.1329 $[\text{M}+\text{NH}_4]^+$, found: 448.1324.

tert-Butyl 2-{2-[(acetylsulfanyl)methyl]-3-[2-(tert-butoxy)-2-oxoethoxy]phenoxy}acetate (7): KSAC (3.39 g, 29.7 mmol) was added to **6** (10.69 g, 24.8 mmol) in acetone (200 mL). The suspension was stirred at RT overnight, during which time the pale yellow suspension turned light brown. TLC indicated that the reaction was complete. The suspension was filtered through a short pad of Celite, and the filtrate was evaporated at reduced pressure to yield a brown solid. The crude product was purified by using silica column chromatography (hexane/ether, 5:1) as a pale yellow oil (6.85 g, 65%). $^1\text{H NMR}$ (300 MHz, CDCl_3): $\delta = 1.46$ (s, 18H), 2.31 (s, 3H), 4.39 (s, 2H), 4.53 (s, 4H), 6.40 (d, $J = 8.4$ Hz, 2H), 7.11 ppm (t, $J = 8.4$ Hz, 1H); $^{13}\text{C NMR}$ (300 MHz, CDCl_3): $\delta = 22.47$, 28.17, 30.42, 66.56, 82.44, 105.37, 114.31, 128.56, 157.24, 167.97, 196.24 ppm; NSI-HRMS: m/z calcd. for $\text{C}_{21}\text{H}_{30}\text{O}_7\text{SNH}_4$: 444.2050 $[\text{M}+\text{NH}_4]^+$, found: 444.2049.

2-[(Acetylsulfanyl)methyl]-3-(carboxymethoxy)phenoxyacetic acid

(8): Trifluoroacetic acid (12.51 mL, 0.161 mol) was added to **7** (6.85 g, 16.1 mmol) in CH_2Cl_2 (200 mL). The pale yellow solution was stirred at RT overnight, during which time the pale yellow solution turned yellow, and TLC indicated that the reaction was complete. Water (200 mL) was added, and the white precipitate formed was collected by filtration. The filtrate was washed with water (2×200 mL) and dried over MgSO_4 . Removal of all solvents gave an off-white solid, which was washed with CH_2Cl_2 . The combined yield of **8** was 4.14 g (82%). $^1\text{H NMR}$ (300 MHz, CD_3OD): $\delta = 2.29$ (s, 3H), 4.36 (s, 2H), 4.68 (s, 4H), 6.55 (d, $J = 8.4$ Hz, 2H), 7.17 ppm (t, $J = 8.4$ Hz, 1H); $^{13}\text{C NMR}$ (300 MHz, CD_3OD): $\delta = 23.09$, 30.13, 66.60, 106.66, 115.41, 129.77, 158.52, 172.384, 198.18 ppm; NSI-HRMS: m/z calcd. for $\text{C}_{13}\text{H}_{14}\text{O}_7\text{SH}$: 315.0533 $[\text{M}+\text{H}]^+$, found: 315.0537; elemental analysis calcd. (%) for $\text{C}_{13}\text{H}_{14}\text{O}_7\text{S}$: C 49.68, H 4.49; found: C 49.77, H 4.57.

2-{2-[(Acetylsulfanyl)methyl]-3-[(2-formylphenyl)carbamoyl]methoxy}phenoxy-N-(2-formylphenyl)acetamide (9): To a suspension of **8** (2.30 g, 7.32 mmol), 2-aminobenzaldehyde (2.21 g, 18.2 mmol) and 2-chloro-1-methylpyridinium iodide (4.50 g, 17.6 mmol) in dry CH_2Cl_2 (150 mL) was added Et_3N (5.05 mL, 35.9 mmol). The mixture was stirred at RT overnight after which TLC indicated that the reac-

tion was complete. Removal of the solvents afforded a yellow solid. The crude product was purified by using silica column chromatography (CH₂Cl₂/ether, 20:1) to yield **9** as a white solid (2.30 g, 60%). ¹H NMR (300 MHz, CD₂Cl₂): δ = 2.19 (s, 3H), 4.70 (s, 4H), 4.86 (s, 2H), 6.67 (d, *J* = 8.4 Hz, 2H), 7.24 (t, *J* = 8.4 Hz, 1H), 7.32 (td, *J* = 7.5, 1.0 Hz, 2H), 7.63–7.69 (m, 2H), 7.76 (dd, *J* = 7.6, 1.6 Hz, 2H), 8.77 (d, *J* = 8.4 Hz, 2H), 9.960 (s, 1H), 9.958 (s, 1H), 11.85 ppm (br, s, 2H); ¹³C NMR (300 MHz, CDCl₃): δ = 22.34, 30.40, 69.25, 107.06, 116.40, 120.64, 123.18, 124.08, 129.29, 136.14, 136.21, 140.05, 156.93, 168.04, 195.26, 195.67 ppm; NSI-HRMS: *m/z* calcd. for C₂₇H₂₄N₂O₅SH: 521.1377 [M+H]⁺; found: 521.1372; elemental analysis calcd. (%) for C₃₅H₃₃Br₂O₅Si₂: C 62.30, H 4.65, N 5.38; found: C 62.44, H 4.53, N 5.25.

5,15-Bis-(2-nitrophenyl)-10,20-bis-(4-iodophenyl)porphyrin (10): To a clear solution of 5-(2-nitrophenyl)-dipyrromethane (5.37 g, 20 mmol) and 4-iodo-benzaldehyde (4.64 g, 20 mmol) in degassed CH₂Cl₂ (2 L) was added TFA (2.80 mL, 35.9 mmol), and the resulting dark red solution was stirred at RT overnight. DDQ (4.77 g, 21 mmol) was then added, and the resulting dark green solution was stirred at RT for 3 h. Et₃N (6.0 mL, 0.0426 mol) was added to the dark green mixture, which was stirred at RT for another 10 min. The black CH₂Cl₂ solution was passed through a neutral alumina column and eluted with CH₂Cl₂. The dark red eluent containing *cis/trans*-isomers was concentrated to afford a dark violet solid (2.13 g, 11%). The solid was pure enough for the next reaction judged by ¹H NMR. ¹H NMR (300 MHz, D₆-DMSO): δ = -2.91 (s, 2H), 7.89–8.02 (m, 3H), 8.10–8.20 (m, 9H), 8.37–8.43 (m, 2H), 8.55–8.59 (m, 2H), 8.74 (d, *J* = 4.7 Hz, 4H), 8.85 ppm (d, *J* = 4.7 Hz, 4H); APCI-HRMS: *m/z* calcd. for C₄₄H₂₆I₂N₆O₄H: 957.0178 [M+H]⁺; found: 957.0158; elemental analysis calcd. (%) for C₄₄H₂₆I₂N₆O₄: C 55.25, H 2.74, N 8.79; found: C 55.37, H 2.63, N 8.69.

***cis*-5,15-Bis-(2-aminophenyl)-10,20-bis-(4-iodophenyl)porphyrin (11):** To a solution of **10** (1.46 g, 1.53 mmol) in concentrated HCl (250 mL) was added SnCl₂ (8.7 g, 0.046 mol). The dark green mixture was stirred at RT for 3 days. TLC indicated that the reaction was complete. The dark green mixture was treated with concentrated NH₃·H₂O at 0–5 °C until pH > 8. To this basic suspension was added EtOAc (250 mL), and the mixture was stirred at RT for 2 h. The EtOAc layer was separated and the aqueous layer was extracted with EtOAc (2 × 200 mL). The combined EtOAc layers were washed with water until the washing had a pH of approximately 8, and then dried over Na₂SO₄. The desired *cis*-isomer was separated from the partially reduced product and *trans*-isomer by using silica column chromatography (CH₂Cl₂ → CH₂Cl₂/EtOAc 100:1) as a dark violet crystalline solid. The isolated *trans*-isomer was heated at 80 °C in toluene with silica, during which time some *trans*-isomer molecules converted to their *cis*-isomers. The *cis*-isomer was separated from *trans*-isomer by using silica column chromatography in the same way as aforementioned. The combined yield was 0.67 g (49%). ¹H NMR (300 MHz, CD₂Cl₂): δ = -2.82 (s, 2H), 3.58 (s, 4H), 7.12–7.19 (m, 4H), 7.61 (td, *J* = 7.7, 1.5 Hz, 2H), 7.84 (dd, *J* = 7.4, 1.4 Hz, 2H), 7.94–7.97 (m, 4H), 8.12 (d, *J* = 8.5 Hz, 4H), 8.85 (d, *J* = 4.8 Hz, 4H), 8.91 ppm (d, *J* = 4.8 Hz, 4H); NSI-HRMS: *m/z* calcd. for C₄₄H₃₀I₂N₆H: 897.0694 [M+H]⁺; found: 897.0694; elemental analysis calcd. (%) for C₄₄H₃₀I₂N₆: C 58.94, H 3.37, N 9.37; found: C 59.05, H 3.25, N 9.27.

5-[2,6-Dimethylphenyl]dipyrromethane (12): 2,6-Dimethyl-benzaldehyde (5.00 g, 37.2 mol) was dissolved in freshly distilled pyrrole (27 mL, 0.381 mol), and the clear solution was degassed for 30 min before TFA (0.30 mL, 3.85 mmol) was added. The light yellow mixture was then stirred at RT for 2 h, during which time the solution

turned dark brown; TLC indicated that the reaction was complete. Aqueous NaOH solution (0.1 M, 100 mL) was added to quench the reaction. The mixture was extracted with EtOAc (3 × 50 mL). The combined organic layers were washed with brine (2 × 150 mL) twice and dried over Na₂SO₄. Removal of the solvents afforded a black oily residue. The crude product was purified by using silica column chromatography (hexane/ether, 5:1). The pure product was obtained by recrystallisation from a solvent mixture of CH₂Cl₂ and hexane as a brownish white solid (2.30 g, 25%). ¹H NMR (300 MHz, CD₂Cl₂): δ = 2.10 (s, 6H), 5.91–5.95 (m, 3H), 6.13 (dd, *J* = 6.0, 2.7 Hz, 2H), 6.66–6.68 (m, 2H), 7.03–7.13 (m, 3H), 8.04 ppm (s, 2H); ¹³C NMR (300 MHz, CD₂Cl₂): δ = 20.77, 39.10, 106.82, 108.81, 116.64, 127.41, 129.88, 131.50, 138.07, 138.25 ppm; APCI-HRMS: *m/z* calcd. for C₁₇H₁₈N₂H: 251.1543 [M+H]⁺; found: 251.1542; elemental analysis calcd. (%) for C₁₇H₁₈N₂: C 81.56, H 7.25, N 11.19; found: C 81.61, H 7.34, N 11.07.

Porphyrin 1(Ac): To a suspension of **11** (0.45 g, 0.502 mmol), **8** (0.20 g, 0.636 mmol) and 2-chloro-1-methylpyridinium iodide (0.32 g, 1.25 mmol) in dry CH₂Cl₂ (450 mL) was added Et₃N (0.25 mL, 1.78 mmol). The mixture was stirred at RT for 4 h after which TLC indicated that the reaction was complete. Removal of the solvents gave rise to a dark violet residue. The crude product was purified by using silica column chromatography (CH₂Cl₂/ether, 20:1) as a dark violet solid (0.41 g, 70%). Crystals for X-ray analysis were grown by ether vapour diffusion into the concentrated CH₂Cl₂ solution of **1(Ac)**. ¹H NMR (300 MHz, CD₂Cl₂): δ = -2.86 (s, 2H), -2.62 (s, 2H), 1.01 (s, 3H), 3.57 (d, *J* = 14.4 Hz, 2H), 3.75 (d, *J* = 14.4 Hz, 2H), 5.67 (d, *J* = 8.4 Hz, 2H), 6.47 (t, *J* = 8.4 Hz, 1H), 7.36 (s, 2H), 7.62–7.65 (br, m, 1H), 7.72–7.80 (m, 4H), 7.90 (td, *J* = 7.9, 1.6 Hz, 2H), 8.00–8.12 (br, m, 5H), 8.63 (dd, *J* = 7.5 Hz, *J* = 1.4 Hz, 2H), 8.66 (dd, *J* = 8.3, 0.9 Hz, 2H), 8.80 (m, 4H), 8.90 ppm (m, 4H); MALDI: *m/z* calcd. for C₅₇H₄₀I₂N₆O₅S: 1174.1 [M]⁺; found: 1174.1; elemental analysis calcd. (%) for C₅₇H₄₀I₂N₆O₅S: C 58.27, H 3.43, N 7.15; found: C 58.42, H 3.34, N 7.16.

5,15-Bis-(2-nitrophenyl)-10,20-bis-(2,6-dimethylphenyl)porphyrin (13): To a solution of **12** (2.30 g, 9.19 mmol) and 2-nitrobenzaldehyde (1.39 g, 9.20 mmol) in degassed CH₂Cl₂ (1 L) was added TFA (1.30 mL, 16.7 mmol). The mixture was stirred at RT overnight. DDQ (3.13 g, 13.8 mmol) was then added to this dark red solution. The resulting dark green solution was stirred at RT for 6 h. Et₃N (3.0 mL, 21.3 mmol) was then added, and the mixture was stirred at RT for another 10 min. The black solution was passed through a neutral alumina column and eluted with CH₂Cl₂. The dark red eluent containing *cis/trans*-isomers was concentrated to afford a dark violet solid (0.81 g, 12%). The desired *cis*-isomer was separated from the *trans*-isomer by using neutral alumina column chromatography (CH₂Cl₂) to afford **13** as a dark violet crystalline solid (0.32 g, 4.6%). ¹H NMR (300 MHz, CDCl₃): δ = -2.50 (s, 2H), 1.85 (s, 6H), 1.91 (s, 6H), 7.43–7.48 (m, 4H), 7.57–7.62 (m, 2H), 7.90–8.00 (m, 4H), 8.21 (dd, *J* = 8.1, 1.8 Hz, 2H), 8.48 (dd, *J* = 7.7, 1.8 Hz, 2H), 8.59 (d, *J* = 4.8 Hz, 4H), 8.65 ppm (d, *J* = 4.8 Hz, 4H); MALDI: *m/z* calcd. for C₄₈H₃₆N₆O₄: 760.3 [M]⁺; found: 760.3; elemental analysis calcd. (%) for C₄₈H₃₆N₆O₄: C 75.77, H 4.77, N 11.05; found: C 75.91, H 4.67, N 10.91.

***cis*-5,15-Bis-(2-aminophenyl)-10,20-bis-(2,6-dimethylphenyl)porphyrin (14):** To a solution of **13** (0.32 g, 0.42 mmol) in concentrated HCl (50 mL) was added SnCl₂ (0.8 g, 4.22 mmol). The dark green mixture was stirred at RT for 20 h. The following TLC indicated that the reaction was complete. The mixture was treated with aqueous KOH solution at 0–5 °C until pH > 8. EtOAc (250 mL) was added to this basic suspension, and the mixture was stirred at RT for 2 h.

The EtOAc layer was separated, and the aqueous layer was extracted with EtOAc (2×200 mL). The combined EtOAc layers were washed with water until the washing had a pH of approximately 8, and then dried over Na₂SO₄. The desired *cis*-isomer was separated from small amounts of *trans*-isomer by using silica column chromatography (CH₂Cl₂/ether, 20:1) as a dark violet crystalline solid (0.17 g, 58%). ¹H NMR (300 MHz, CD₂Cl₂): δ = -2.61 (s, 2H), 1.84 (s, 6H), 1.91 (s, 6H), 3.65 (s, 4H), 7.11–7.18 (m, 4H), 7.46–7.50 (m, 4H), 7.56–7.64 (m, 4H), 7.86 (dd, *J* = 7.4, 1.4 Hz, 2H), 8.66 (d, *J* = 4.8 Hz, 4H), 8.85 ppm (d, *J* = 4.8 Hz, 4H). ESI-HRMS: *m/z* calcd. for C₄₈H₄₀N₆: 700.3 [M]⁺; found: 700.3; elemental analysis calcd. (%) for C₄₈H₄₀N₆: C 82.26, H 5.75, N 11.99; found: C 78.54, H 5.76, N 10.18.

Porphyrin 2(Ac): To a suspension of **14** (0.16 g, 0.228 mmol), **8** (90 mg, 0.286 mmol) and 2-chloro-1-methylpyridinium iodide (0.15 g, 0.587 mmol) in dry CH₂Cl₂ (220 mL) was added Et₃N (0.16 mL, 1.13 mmol). The mixture was stirred at RT overnight. The following TLC indicated that the reaction was complete. Removal of the solvents gave rise to dark violet residue. The crude product was purified by using silica column chromatography (CH₂Cl₂, then CH₂Cl₂/ether, 50:1→20:1) to afford **2(Ac)** as a dark violet solid (0.16 g, 72%). Crystals for X-ray analysis were grown by ether vapour diffusion into the concentrated CH₂Cl₂ solution of **2(Ac)**. ¹H NMR (300 MHz, CD₂Cl₂): δ = -2.75 (s, 2H), -2.41 (s, 2H), 0.942 (s, 3H), 1.01 (s, 3H), 1.58 (s, 3H), 1.73 (s, 3H), 2.25 (s, 3H), 3.57 (d, *J* = 14.3 Hz, 2H), 3.84 (d, *J* = 14.3 Hz, 2H), 5.76 (d, *J* = 8.4 Hz, 2H), 6.56 (t, *J* = 8.4 Hz, 1H), 7.29 (d, *J* = 7.6 Hz, 1H), 7.36–7.42 (m, 2H), 7.52 (t, *J* = 7.6 Hz, 1H), 7.57–7.64 (m, 4H), 7.75 (td, *J* = 7.5, 1.3 Hz, 2H), 7.88 (td, *J* = 7.8, 1.6 Hz, 2H), 8.53 (d, *J* = 4.8 Hz, 2H), 8.60 (dd, *J* = 8.2, 0.99 Hz, 2H), 8.66 (dd, *J* = 7.5, 1.5 Hz, 2H), 8.70 (d, *J* = 4.8 Hz, 2H), 8.73 (d, *J* = 4.8 Hz, 2H), 8.83 ppm (d, *J* = 4.7 Hz, 2H); NSI-HRMS: *m/z* calcd. for C₆₁H₅₀N₆O₅SH: 979.3636 [M+H]⁺; found: 979.3636; C₆₁H₅₀N₆O₅Na: 1001.3461 [M+Na]⁺; found: 1001.3450.

1,3-Bis[(2-methoxyethoxy)methoxy]benzene (15): To a solution of resorcinol (10.00 g, 90.8 mmol) in dry DMF (160 mL) was added NaH (60% dispersion in mineral oil, 8.72 g, 0.218 mol) portion by portion at 0–5 °C. The off-white suspension was stirred at RT for 2 h. The suspension was cooled to 0–5 °C again, followed by slow addition of MEMCl (22.60 mL, 0.199 mol). The mixture was warmed to RT and stirred overnight; TLC indicated that the reaction was complete. Aqueous NaHCO₃ solution (0.5 M, 200 mL) was added slowly to quench the reaction. The mixture was extracted with EtOAc (1×200 mL, 2×100 mL). The combined organic layers were washed with brine twice (2×400 mL) and dried over MgSO₄. Removal of the solvents afforded an oily residue. The crude product was purified by using silica column chromatography (EtOAc/hexane, 1:3) to yield **15** as a colourless oil (17.50 g, 67%). ¹H NMR (300 MHz, CDCl₃): δ = 3.40 (br, s, 6H), 3.54–3.57 (m, 4H), 3.80–3.83 (m, 4H), 5.25 (s, 4H), 6.70–6.75 (m, 3H), 7.13 ppm (t, *J* = 8.3 Hz, 1H); ¹³C NMR (300 MHz, CDCl₃): δ = 59.17, 67.81, 71.74, 93.63, 105.22, 109.78, 130.08, 158.47 ppm; ESI-HRMS: *m/z* calcd. for C₁₄H₂₂O₆Na: 309.1309 [M+Na]⁺; found: 309.1310.

2,6-Bis[(2-methoxyethoxy)methoxy]benzaldehyde (16): To a solution of **15** (7.50 g, 26.2 mmol) in dry degassed THF (120 mL) was added *n*BuLi (1.6 M in hexane, 18.00 mL, 0.288 mol) at 0–5 °C. The yellow solution was stirred for 45 min before dry DMF (4.0 mL, 0.0517 mol) was added at 0–5 °C. The light yellow mixture was warmed to RT and stirred for 2 h after which TLC indicated that the reaction was complete. Aqueous HCl solution (0.1 M, 150 mL) was added slowly to quench the reaction. The mixture was extracted with EtOAc (1×150 mL, 2×100 mL). The combined organic layers were washed with brine twice (2×350 mL) and dried over MgSO₄.

Removal of the solvents gave rise to an oily residue which was purified by silica column chromatography (CH₂Cl₂/ether, 5:1) to afford **16** as a colourless oil (4.75 g, 58%). ¹H NMR (300 MHz, CDCl₃): δ = 3.37 (br, s, 6H), 3.54–3.57 (m, 4H), 3.84–3.87 (m, 4H), 5.35 (s, 4H), 6.88 (d, *J* = 8.4 Hz, 2H), 7.40 (t, *J* = 8.4 Hz, 1H), 10.51 ppm (s, 1H); ¹³C NMR (300 MHz, CDCl₃): δ = 59.16, 68.30, 71.62, 93.95, 108.81, 116.24, 135.74, 159.52, 189.39 ppm; ESI-HRMS: *m/z* calcd. for C₁₅H₂₂O₇Na: 337.1258 [M+Na]⁺; found: 337.1259.

2-[(2,6-Bis[(2-methoxyethoxy)methoxy]phenyl)(1 *H*-pyrrol-2-yl)-methyl]-1 *H*-pyrrole (17): Compound **16** (4.65 g, 0.0148 mol) was dissolved in freshly distilled pyrrole (27 mL, 0.381 mol). The clear solution was degassed for 30 min before addition of TFA (0.12 mL, 1.54 mmol). The light yellow mixture was stirred at RT for 10 min, during which time the light yellow solution turned to dark brown. The following TLC indicated that the reaction was complete. Aqueous NaOH solution (0.1 M, 100 mL) was added to quench the reaction. The mixture was extracted with EtOAc (3×50 mL). The combined organic layers were washed with brine twice (2×150 mL) and dried over Na₂SO₄. Removal of the solvents gave rise to a black oily residue. The crude product was purified by using silica column chromatography (CH₂Cl₂/ether, 10:1) as a pale yellow oil (2.47 g, 39%). ¹H NMR (300 MHz, CDCl₃): δ = 3.37 (br, s, 6H), 3.50–3.52 (m, 4H), 3.65 (br, s, 4H), 5.17 (br, s, 4H), 5.937–5.939 (m, 2H), 6.63–6.65 (m, 2H), 6.84 (d, *J* = 8.3 Hz, 2H), 7.16 ppm (t, *J* = 8.3 Hz, 1H); ¹³C NMR (300 MHz, CDCl₃): δ = 33.21, 59.15, 68.00, 71.76, 94.13, 106.27, 107.99, 109.63, 116.37, 121.30, 128.46, 132.81, 155.69 ppm; ESI-HRMS: *m/z* calcd. for C₂₃H₃₀N₂O₆Na: 453.1996 [M+Na]⁺; found: 453.1993.

Porphyrin 3(Ac): To a clear solution of dipyrromethane **17** (0.25 g, 0.58 mmol) and dialdehyde **9** (0.15 g, 0.288 mmol) in degassed CH₂Cl₂ (100 mL) was added TFA (0.15 mL, 1.92 mmol). The mixture was stirred at RT overnight. To this very dark pink solution was then added DDQ (0.25 g, 1.10 mmol). The resulting dark greenish solution was stirred at RT for 3 h before Et₃N (0.30 mL, 2.13 mmol) was added. The black mixture was stirred for 30 min, and then passed through a short neutral alumina column, which was washed initially with CH₂Cl₂, then CH₂Cl₂/THF (1:1). The concentrated black eluent was purified by using silica column chromatography (EtOAc/CH₂Cl₂, 1:1 to 1.5:1) to yield a dark violet solid (9 mg, 2.3%). The dark violet crystals for X-ray analysis were obtained by ether vapour diffusion into the concentrated CH₂Cl₂ solution of **3(Ac)**. ¹H NMR (300 MHz, CDCl₃): δ = -2.60 (s, 2H), -2.37 (s, 2H), 0.52 (s, 3H), 2.70–2.75 (m, 4H), 2.86–3.01 (m, 12H), 3.22–3.29 (m, 8H), 3.36–3.39 (m, 2H), 3.51–3.54 (m, 2H), 3.65 (d, *J* = 14.1 Hz, 2H), 3.84 (d, *J* = 14.1 Hz, 2H), 4.05 (s, 2H), 4.60 (s, 2H), 4.75 (s, 2H), 5.23 (s, 2H), 5.78 (d, *J* = 8.4 Hz, 2H), 6.55 (t, *J* = 8.4 Hz, 1H), 7.13–7.21 (m, 3H), 7.42 (d, *J* = 8.1 Hz, 2H), 7.63–7.77 (m, 6H), 7.12 (td, *J* = 7.9, 1.6 Hz, 2H), 8.67–8.73 (m, 8H), 8.87 ppm (m, 4H); MALDI: *m/z* calcd. for C₇₃H₇₄N₆O₁₇S: 1138.5 [M]⁺; found: 1138.4.

Porphyrin 4(Ac): To a clear solution of 5-(pentafluorophenyl)dipyrromethane (0.56 g, 1.79 mmol) and dialdehyde **9** (0.47 g, 0.90 mmol) in degassed CH₂Cl₂ (320 mL) was added TFA (0.47 mL, 6.03 mmol). The mixture was stirred at RT overnight. To this very dark pink solution DDQ (0.80 g, 3.52 mmol) was added. The resulting dark greenish solution was stirred at RT for 7 h before Et₃N (0.50 mL, 3.55 mmol) was added. The black mixture was stirred for 30 min and then passed through a short neutral alumina column, which was washed initially with CH₂Cl₂, then CH₂Cl₂/THF (1:1). The concentrated black eluent was purified by using silica column chromatography (CH₂Cl₂/ether, 100:1) to yield a dark violet solid (65 mg, 6.6%). Dark violet crystals for X-ray analysis were obtained

by vapour diffusion of ether into the concentrated CH_2Cl_2 solution of **4(Ac)**. $^1\text{H NMR}$ (300 MHz, CD_2Cl_2): δ -2.98 (s, 2H), -2.69 (s, 2H), 0.856 (s, 1H), 0.859 (s, 1H), 3.60 (d, $J=14.3$ Hz, 2H), 3.77 (d, $J=14.3$ Hz, 2H), 5.69 (d, $J=8.4$ Hz, 2H), 6.50 (t, $J=8.4$ Hz, 1H), 7.43 (s, 2H), 7.79 (td, $J=7.5, 1.2$ Hz, 2H), 7.93 (td, $J=7.9, 1.5$ Hz, 2H), 8.62 (dd, $J=8.2, 0.9$ Hz, 2H), 8.65 (dd, $J=7.5, 1.5$ Hz, 2H), 8.75 – 8.77 (m, 2H), 8.87 – 8.91 (m, 4H), 9.03 – 9.04 ppm (m, 2H); NSI-HRMS: m/z calcd. for $\text{C}_{57}\text{H}_{32}\text{F}_{10}\text{N}_6\text{O}_5\text{SH}$: 1103.2068 $[\text{M}+\text{H}]^+$; found: 1103.2043; $\text{C}_{57}\text{H}_{32}\text{F}_{10}\text{N}_6\text{O}_5\text{SNa}$: 1125.1893 $[\text{M}+\text{Na}]^+$; found: 1125.1854.

Fe-1: Porphyrin **1(Ac)** (60 mg, 511 μmol), FeBr_2 (110 mg, 0.511 mmol) and lutidine (0.10 mL) were added to dry degassed toluene (30 mL). The suspension was refluxed overnight. The ensuing TLC indicated that the reaction was complete. To this cooled suspension was added 0.2 M NaOMe (10 mL). The mixture was stirred at RT for 2 h before it was poured into a mixture of 0.1 M HCl (100 mL) and toluene (20 mL). The toluene layer was separated, washed with water twice (2×50 mL) and dried over Na_2SO_4 . Removal of the solvents under vacuo resulted in a dark solid residue. The crude product was purified by using silica column chromatography (CH_2Cl_2 , then hexane/THF, 1:1) to yield a brown-red solid (38 mg, 63%) after all the solvents were evaporated under vacuo. The brown-red solid was dried under vacuo and re-dissolved in dry degassed CH_2Cl_2 (2 mL). The concentrated dark red CH_2Cl_2 solution was then layered with hexane (3 mL) under N_2 to produce a microcrystalline dark brown-red solid. MALDI: m/z calcd. for $\text{C}_{55}\text{H}_{35}\text{Fe}_2\text{N}_6\text{O}_4\text{S}$: 1185.0 $[\text{M}]^+$; found: 1185.0.

Fe-2: Porphyrin **2(Ac)** (40 mg, 40.8 μmol), FeBr_2 (90 mg, 0.417 mmol) and lutidine (0.10 mL) were added to dry degassed toluene (30 mL). The suspension was refluxed overnight. The ensuing TLC indicated the reaction was complete. To this cooled suspension was added NaOMe (0.2 M, 10 mL). The mixture was stirred at RT for 2 h before it was poured into a mixture of HCl (0.1 M, 100 mL) and toluene (20 mL). The toluene layer was separated, washed with water twice (2×50 mL) and dried over Na_2SO_4 . Removal of the solvents under vacuo gave a dark solid residue. The crude product was purified by using silica column chromatography (CH_2Cl_2 , then $\text{CH}_2\text{Cl}_2/\text{THF}$, 50:1) to yield a red-brown solid (25 mg, 61%) after all the solvents were evaporated under vacuo. The red-brown solid was dried under vacuo and re-dissolved in dry degassed CH_2Cl_2 (3 mL). The concentrated dark red CH_2Cl_2 solution was then layered with degassed hexane (4 mL) under N_2 to give microcrystalline dark red-brown solid. MALDI: m/z calcd. for $\text{C}_{59}\text{H}_{45}\text{FeN}_6\text{O}_4\text{S}$: 989.3 $[\text{M}]^+$; found: 989.3.

Fe-3: Porphyrin **3(Ac)** (30 mg, 22.4 μmol), FeBr_2 (50 mg, 0.232 mmol) and lutidine (0.10 mL) were added to dry degassed toluene (25 mL). The suspension was refluxed overnight. The ensuing TLC indicated that the reaction was complete. To this cooled suspension was added NaOMe (0.2 M, 10 mL). The mixture was stirred at RT for 2 h before it was poured into a mixture of HCl (0.1 M, 100 mL) and toluene (25 mL). The toluene layer was separated, washed with water twice (2×50 mL) and dried over Na_2SO_4 . Removal of the solvents under vacuo produced a dark solid residue. The crude product was purified by using silica column chromatography (CH_2Cl_2 , then $\text{CH}_2\text{Cl}_2/\text{THF}$, 20:1) to yield a brown-red solid after all the solvents were evaporated under vacuo. The brown-red solid was dried under vacuo and re-dissolved in dry degassed CH_2Cl_2 (2 mL). The concentrated dark red CH_2Cl_2 solution was then layered with hexane (4 mL) under N_2 to yield dark violet needles (16 mg, 53%). MALDI: m/z calcd. for $\text{C}_{71}\text{H}_{69}\text{N}_6\text{O}_{16}\text{SFe}$: 1149.4 $[\text{M}]^+$; found: 1149.4.

Fe-4: Porphyrin **4(Ac)** (30 mg, 27.2 μmol), FeBr_2 (60 mg, 0.278 mmol) and lutidine (0.10 mL) were added to dry degassed toluene (25 mL). The suspension was refluxed overnight. The ensuing TLC indicated that the reaction was complete. To this cooled suspension was added NaOMe (0.2 M, 10 mL). The mixture was stirred at RT for 2 h before it was poured into a mixture of HCl (0.1 M, 100 mL) and toluene (25 mL). The toluene layer was separated, washed with water twice (2×50 mL) and dried over Na_2SO_4 . Removal of the solvents under vacuo resulted in a dark solid residue. The crude product was purified by using silica column chromatography (CH_2Cl_2 , then $\text{CH}_2\text{Cl}_2/\text{THF}$, 50:1) to yield a brown-red solid (15 mg, 50%) after all the solvents were evaporated under vacuo. The brown-red solid was dried under vacuo and re-dissolved in dry degassed CH_2Cl_2 (3 mL). The concentrated dark red CH_2Cl_2 solution was then layered with hexane (5 mL) under N_2 to yield a dark brown-red solid, which was collected and dried under vacuo. MALDI: m/z calcd. for $\text{C}_{55}\text{H}_{27}\text{F}_{10}\text{FeN}_6\text{O}_4\text{S}$: 1113.1 $[\text{M}]^+$; found: 1113.1.

X-ray crystallography

For each sample, crystals were suspended in oil, and one was mounted on a glass fibre and fixed in the cold nitrogen stream of the diffractometer. Data were collected by recording synchrotron radiation ($\lambda=0.6889$) using a Rigaku Saturn724+ diffractometer equipped with confocal monochromator [**1(Ac)**] or MoK_α ($\lambda=0.71073$ Å) radiation using an Oxford Diffraction Xcalibur-3 CCD diffractometer equipped with a graphite monochromator [**3(Ac)** and **4(Ac)**] or a Bruker-Nonius Apex II diffractometer equipped with confocal mirrors [(thf)Fe-1·(thf)·(CH_2Cl_2)]. Data were processed by using the CrystalClear SM Expert [**1(Ac)**],^[22a] CrysAlisPro [**3(Ac)** and **4(Ac)**]^[22b] or DENZO and COLLECT [(thf)Fe-1·(thf)·(CH_2Cl_2)] software.^[22c] Structures were determined by the direct methods routines in SIR92 [**1(Ac)** and **4(Ac)**],^[22d] SHELXS [**3(Ac)**]^[22e] or SIR97 [(thf)Fe-1·(thf)·(CH_2Cl_2)]^[22f] programmes and refined by full-matrix least-squares methods on F^2 in SHELXL.^[22e] Non-hydrogen atoms were refined with anisotropic thermal parameters. Hydrogen atoms H(1), H(21), H(167) and H(367) were freely refined in **3(Ac)**, whereas all other hydrogen atoms were included in idealised positions and their U_{iso} values were set to ride on the U_{eq} values of the parent carbon or nitrogen atom. In [(thf)Fe(1)·(thf)·(CH_2Cl_2)] and **1(Ac)**, disordered solvent regions were handled using the SQUEEZE procedure.^[22g] A summary of the crystallographic data for previously unreported structures is given in Table 4. CCDC 886113 to CCDC 886116 contain the supplementary crystallographic data for **1(Ac)**, **3(Ac)**, **4(Ac)** and [(thf)Fe-1·(thf)·(CH_2Cl_2)], respectively. These data can be obtained free of charge from The Cambridge Crystallographic Data Centre via www.ccdc.cam.ac.uk/data_request/cif.

Acknowledgements

We thank the EPSRC and our colleagues in the SolarCAP consortium (EPSRC F047878/1) for supporting this work. K.A. thanks the University of Hail, Saudi Arabia, for providing a Scholarship. The authors thank the EPSRC National Mass Spectrometry Service, Swansea, for mass spectroscopy data, and the EPSRC National Crystallography Service for collection of diffraction data.^[23]

Keywords: electrocatalysis · hydrocarbons · iron · oxidation · porphyrins

Table 4. Crystallographic Data for 1(Ac), 3(Ac), 4(Ac) and Fe-1.

Property	1(Ac)	3(Ac)	4(Ac)	[(thf)Fe-1·(thf)·(CH ₂ Cl ₂)]
formula	C ₅₇ H ₄₀ I ₂ N ₆ O ₅ S	C ₇₃ H ₇₄ N ₆ O ₁₇ S	C ₅₇ H ₃₂ F ₁₀ N ₆ O ₅ S	C ₅₉ H ₄₃ FeI ₂ N ₆ O ₅ S, C ₄ H ₈ O, CH ₂ Cl ₂
molecular weight [g cm ⁻³]	1174.81	1339.44	1102.95	1414.73
crystal system	monoclinic	triclinic	triclinic	triclinic
space group	<i>P</i> 2 ₁ / <i>n</i>	<i>P</i> 1	<i>P</i> 1	<i>P</i> 1
crystal description, colour	block, red	sliver, red-brown	prism, dark purple	plate, brown
crystal dimensions [mm]	0.02 × 0.03 × 0.05	0.15 × 0.24 × 0.25	0.17 × 0.20 × 0.35	0.01 × 0.09 × 0.14
<i>a</i> [Å]	13.292(5)	13.5315(9)	10.7867(3)	12.4593(5)
<i>b</i> [Å]	28.413(10)	13.6265(9)	14.5984(4)	17.4383(9)
<i>c</i> [Å]	14.958(5)	19.5980(12)	17.4320(5)	18.0032(8)
<i>α</i> [°]	90	103.138(5)	70.899(2)	107.406(2)
<i>β</i> [°]	109.105(5)	100.302(5)	85.460(2)	107.097(2)
<i>γ</i> [°]	90	104.542(6)	70.258(3)	101.066(3)
<i>V</i> [Å ³]	5338(3)	3297.9(4)	2439.88(12)	3395.3(3)
<i>Z</i>	4	2	2	2
<i>ρ</i> _{calc} [g cm ⁻³]	1.459	1.349	1.501	1.384
2 θ _{max} [°]	48.42	50.0	50.00	50.00
<i>T</i> [K]	120(2)	140(1)	140(2)	120(2)
data collected/unique	41 081/9358	44 388/11 576	31 261/8572	53 971/11 894
'observed' reflections (<i>i</i> > 2 σ)	7686	6475	6284	7325
μ [mm ⁻¹]	1.270	0.127	0.164	1.291
<i>R</i> ₁ (<i>I</i> > 2 σ)	0.080	0.042	0.049	0.106
<i>wR</i> ₂ (all data)	0.219	0.089	0.124	0.274
largest diff. peak and hole	2.93, -1.42	0.27, -0.30	0.54, -0.39	1.63, -1.98

- [1] a) C.-M. Che, V. K.-L. Lo, C.-Y. Zhou, J.-S. Huang, *Chem. Soc. Rev.* **2011**, *40*, 1950–1975; b) D. Mansuy, *C. R. Chim.* **2007**, *10*, 392–413; c) B. Meunier, A. Robert, G. Pratiel, J. Bernadou in *The Porphyrin Handbook*, Vol. 4 (Eds.: K. M. Kadish, K. M. Smith, R. Guilard), Academic Press, London, **2000**, pp. 119–187; d) B. Meunier, *Chem. Rev.* **1992**, *92*, 1411–1456; e) J. T. Groves, T. E. Nemo, R. S. Myers, *J. Am. Chem. Soc.* **1979**, *101*, 1032–1033.
- [2] A. Nanthakumar, H. M. Goff, *J. Am. Chem. Soc.* **1990**, *112*, 4047–4049.
- [3] J. T. Groves, J. A. Gilbert, *Inorg. Chem.* **1986**, *25*, 123–125.
- [4] a) T. L. Poulos, B. C. Finzel, I. C. Gunsalus, G. C. Wagner, J. Kraut, *J. Biol. Chem.* **1985**, *260*, 16122–16130; b) K. G. Ravichandran, S. S. Boddupalli, C. A. Hasermann, J. A. Peterson, J. Deisenhofer, *Science* **1993**, *261*, 731–736.
- [5] J. E. Baldwin, T. Klose, M. Peters, *Chem. Commun.* **1976**, 881–883.
- [6] a) A. R. Battersby, W. Howson, A. D. Hamilton, *Chem. Commun.* **1982**, 1266–1268; b) H.-A. Wagenknecht, W.-D. Woggon, *Angew. Chem.* **1997**, *109*, 404–407; *Angew. Chem. Int. Ed. Engl.* **1997**, *36*, 390–392; c) H. Volz, M. Holzbecher, *Angew. Chem.* **1997**, *109*, 1510–1513; *Angew. Chem. Int. Ed. Engl.* **1997**, *36*, 1442–1445; d) H.-A. Wagenknecht, C. Claude, W.-D. Woggon, *Helv. Chim. Acta* **1998**, *81*, 1506–1520.
- [7] a) J. H. Dawson, *Science* **1988**, *240*, 433–439; b) J. T. Groves, *J. Inorg. Biochem.* **2006**, *100*, 434–447; c) J. Rittle, M. T. Green, *Science* **2010**, *330*, 933–937; d) B. Meunier, S. P. de Visser, S. Shaik, *Chem. Rev.* **2004**, *104*, 3947–3980.
- [8] a) J. M. Mayer, *Acc. Chem. Res.* **1998**, *31*, 441–450; b) M. T. Green, *Curr. Opin. Chem. Biol.* **2009**, *13*, 84–88.
- [9] J. Manka, D. S. Lawrence, *Tetrahedron Lett.* **1989**, *30*, 6989–6992.
- [10] The crystals for X-ray analysis were grown in a solvent mixture containing THF, dichloromethane, and hexane. Hence, the sixth coordination site of iron was occupied by THF. The solid sample for catalysis was prepared in solvent mixture of CH₂Cl₂ and hexane. It is very likely that the iron centre is five-coordinated.
- [11] N. Suzuki, T. Higuchi, Y. Urano, K. Kikuchi, H. Uekusa, Y. Ohashi, T. Uchida, T. Kitagawa, T. Nagano, *J. Am. Chem. Soc.* **1999**, *121*, 11571–11572.
- [12] M. A. Phillippi, H. M. Goff, *J. Am. Chem. Soc.* **1982**, *104*, 6026–6034.
- [13] a) J. T. Groves, T. E. Nemo, *J. Am. Chem. Soc.* **1983**, *105*, 6243–6248; b) M. J. Nappa, C. A. Tolman, *Inorg. Chem.* **1985**, *24*, 4711–4719; c) J. F. Bartoli, O. Brigaud, P. Battioni, D. Mansuy, *Chem. Commun.* **1991**, 440–442.
- [14] a) D. Dolphin, T. G. Traylor, L. Y. Xie, *Acc. Chem. Res.* **1997**, *30*, 251–259; b) H. Fujii, *J. Am. Chem. Soc.* **1993**, *115*, 4641–4648.
- [15] M. das Dores Assis, J. R. L. Smith, *J. Chem. Soc. Perkin Trans. 2* **1998**, 2221–2226.
- [16] T. Higuchi, K. Shimada, N. Maruyama, M. Hirobe, *J. Am. Chem. Soc.* **1993**, *115*, 7551–7552.
- [17] W. H. Koppenol, J. F. Liebman, *J. Phys. Chem.* **1984**, *88*, 99–101.
- [18] H. Saltzman, J. G. Sharefkin, *Org. Synth.* **1963**, *43*, 60–61.
- [19] K. Calderon-Kawasaki, S. Kularatne, Y. H. Li, B. C. Noll, W. R. Scheidt, D. H. Burns, *J. Org. Chem.* **2007**, *72*, 9081–9087.
- [20] J. M. Tour, A. M. Rawlett, M. Kozaki, Y. X. Yao, R. C. Jagessar, S. M. Dirk, D. W. Price, M. A. Reed, C. W. Zhou, J. Chen, W. Y. Wang, I. Campbell, *Chem. Eur. J.* **2001**, *7*, 5118–5134.
- [21] A. Osuka, G. Noya, S. Taniguchi, T. Okada, Y. Nishimura, I. Yamazaki, N. Mataga, *Chem. Eur. J.* **2000**, *6*, 33–46.
- [22] a) *CrystalClear-SM Expert*, version 2.0 r7, Rigaku Europe, Sevenoaks, UK, **2010**; b) *CrysAlisPro*, Oxford Diffraction Ltd., Abingdon, UK, **2010**; c) Z. Otwinowski, W. Minor in *Methods in Enzymology*, Vol. 276 (Eds.: C. W. Carter Jr., R. M. Sweet), Academic Press, **1997**, pp. 307–326; d) A. Altomare, G. Cascarano, C. Giacovazzo, A. Guagliardi, *J. Appl. Crystallogr.* **1993**, *26*, 343–350; e) G. M. Sheldrick, *Acta Crystallogr. Sect. A* **2008**, *64*, 112–122; f) A. Altomare, M. C. Burla, M. Camalli, G. L. Cascarano, C. Giacovazzo, A. Guagliardi, A. G. G. Moliterni, G. Polidori, R. Spagna, *J. Appl. Crystallogr.* **1999**, *32*, 115–119; g) P. van der Sluis, A. L. Spek, *Acta Crystallogr. Sect. A* **1990**, *46*, 194–201.
- [23] S. J. Coles, P. A. Gale, *Chem. Sci.* **2012**, *3*, 683–689.

Received: August 7, 2012

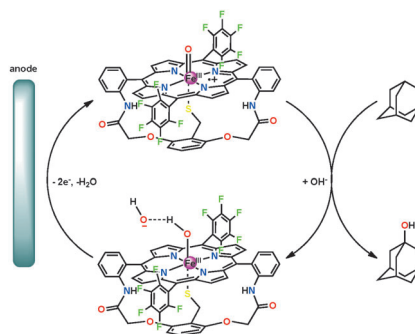
Published online on ■■■■■, 0000

FULL PAPERS

P. Li, K. Alenezi, S. K. Ibrahim, J. A. Wright,
D. L. Hughes, C. J. Pickett*



Towards Alternatives to Anodic Water Oxidation: Basket-Handle Thiolate Fe^{III} Porphyrins for Electrocatalytic Hydrocarbon Oxidation



A preference for alcohol over oxygen:
We show that iron porphyrins can mediate the anodic oxidation of hydrocarbons, thus providing a potential complementary reaction to cathodic generation of fuels or feedstocks as an alternative to oxygen evolution.